HIGHWAY RESEARCH RECORD

Number 123

Highway Drainage and Scour Studies

3 Reports

Subject Classification

23 Highway Drainage
27 Bridge Design

HIGHWAY RESEARCH BOARD

DIVISION OF ENGINEERING NATIONAL RESEARCH COUNCIL
NATIONAL ACADEMY OF SCIENCES—NATIONAL ACADEMY OF ENGINEERING

Washington, D. C., 1966 Publication 1365

Department of Design

W. B. Drake, Chairman
Assistant State Highway Engineer for Planning, Research and Materials
Kentucky Department of Highways, Lexington

HIGHWAY RESEARCH BOARD STAFF

F. N. Wray, Engineer of Design
R. C. Edgerton, Assistant Engineer of Design

GENERAL DESIGN DIVISION

M. D. Shelby, Chairman
Research Engineer, Texas Transportation Institute
Texas A & M University, College Station

COMMITTEE ON SURFACE DRAINAGE OF HIGHWAYS
(As of December 31, 1965)

Carl F. Izzard, Chairman
Science Advisor, Program Analysis Group
Office of Research and Development, U. S. Bureau of Public Roads
Washington, D. C.

R. C. Edgerton, Hydrographic Engineer, North Carolina State Highway Commission, Raleigh
Kenneth S. Eff, Chief, Hydraulic Section, Civil Engineering Branch, Office, Chief of Engineers, Department of the Army, Washington, D. C.
Kenneth M. Fenwick, Assistant Engineer of Design, California Division of Highways, Sacramento
John G. Hendrickson, Jr., Water Resources Bureau, Portland Cement Association, Chicago, Illinois
S. W. Jens, Consulting Engineer, St. Louis, Missouri
Frank L. Johnson, Hydraulic Engineer, Region 6, U. S. Bureau of Public Roads, Fort Worth, Texas
A. H. Koepf, Consulting Engineer, Orinda, California
Robert A. Norton, Engineer of Hydraulics & Bridge Maintenance, Connecticut State Highway Department, Wethersfield
Ralph M. Peterson, Chief, Branch of Management Studies and Systems Planning, Forest Service, U. S. Department of Agriculture, Washington, D. C.
A. L. Pond, Jr., Hydraulic Engineer, Virginia Department of Highways, Richmond
W. O. Ree, Agricultural Research Service, Stillwater, Oklahoma
James K. Searcy, Hydraulic Engineer, Hydraulic Branch, Bridge Division, U. S. Bureau of Public Roads, Washington, D. C.
E. P. Sellner, Hind Engineering Company, Highland Park, Illinois
Roy E. Smith, Managing Director, National Corrugated Steel Pipe Association, Chicago, Illinois
William P. Somers, Assistant Chief, Hydraulics Section, Surface Water Branch, U. S. Geological Survey, Washington, D. C.
F. W. Thorstenson, Assistant Road Design Engineer, Minnesota Department of Highways, St. Paul
Mainard Wacker, Chief Highway Designer (Hydraulics), Hydraulics Section, Advance Plans Division, Wyoming Highway Department, Cheyenne

Foreword

The papers in this Record represent very different applications of hydraulics to highway problems and consequently will be of interest to engineers involved in the design of highway drainage facilities.

Dr. Anderson's paper will be of special interest to those responsible for bridge foundations. He reports on a study of a bridge collapse that was initiated by the undermining by erosion of one of the piers. The study, which included field investigations and model tests, resulted in recommendations for the security of both the replacement structure and the parallel structure which remained in place.

By a series of model studies, Behlke and Pritchett have developed methods for predicting the wall pile-up height of diagonal waves produced at supercritical flow channel junctions. They also suggest design features that eliminate diagonal waves downstream from the junction. Their work will have direct application in the design of lined roadside channels and channel changes on steep slopes.

In the third paper, Dr. Cassidy reports on the hydraulic efficiency of a series of different grate inlet configurations. The results are presented in generalized graphical fashion and will have application in many cases of storm drain inlet design.

Contents

The Hydraulic Design of Bridges for River Crossings—A Case History

ALVIN G. ANDERSON, University of Minnesota, St. Anthony Falls Hydraulic Laboratory

Following collapse of one of the I-29 bridges on April 1, 1962, a model study was performed to define hydraulic conditions that led to collapse and to test proposed protective works. The collapse was initiated by the undermining by erosion of one of the piers of the upstream bridge. A consequence of the erosion pattern was the subsidence of a portion of the left bank, which was left without support when the bed downstream of the bridges eroded to a considerable depth.

The erosion pattern was the result of at least four factors: (1) a flood discharge 1.64 times as large as the maximum flood prior to the design of the bridge was conducive to high velocities through the bridge section; (2) cohesiveness of the riverbed effectively prevented the formation of bed load because when the cohesive bond was broken the bed material went into suspension; (3) the low stage in the Missouri River was favorable to a still higher increase in velocity; and (4) the bridge geometry provided constriction and obstruction to flow and piers were skewed to direction of flow.

The proposal for stabilization of the left bank and prevention from further subsidence incorporated revetment protection for the bridge piers, which had been reconstructed with extensive foundation piles. Hydraulic model tests established the flow and erosion patterns resulting from the revised revetment and showed that the stabilization proposal would not be detrimental to the flow pattern through the bridge structure.

•THE I-29 highway leading from Iowa into South Dakota crosses the Big Sioux River about a mile and a half upstream of its confluence with the Missouri River near Sioux City, Iowa. At this point the river makes an approximate right-angle bend. Just upstream of the bend, two parallel bridges were constructed which crossed the river at an angle to the main flow in the channel. They were supported on webbed piers spaced 120 ft apart. The piers were numbered from the west (South Dakota) side beginning with the abutment so that the first pier from the west is designated as pier 2. Piers 3 and 4 for each bridge were founded on the river bottom proper. At normal flow the river was about 250 ft wide and with the mean bed level at about elevation 1071 ft. The footings of the piers at elevation 1066 ft were supported by piles 25 to 34 ft long.

On April 1, 1962, during a flood, the upstream bridge of the pier collapsed. The initial failure occurred about 3:30 a.m. and from the evidence available it appears to have been the result of the undermining of pier 3 (Fig. 1). This in turn resulted in the rupture of the adjacent spans with the consequent failure of pier 4 about 12 hr later. An outstanding hydraulic characteristic of the failure aside from the undermining of pier 3 was the development of a very deep and extensive scour hole downstream of the structure. In this area the bed scoured to a depth of approximately 40 ft, which was considerably deeper than the section at the bridge centerline.

Paper sponsored by Committee on Surface Drainage of Highways and presented at the 45th Annual Meeting.

Figure 1. Upstream I-29 bridge after collapse of pier 3 and before collapse of pier 4; river flow is from left to right. (Photo courtesy South Dakota Department of Highways)

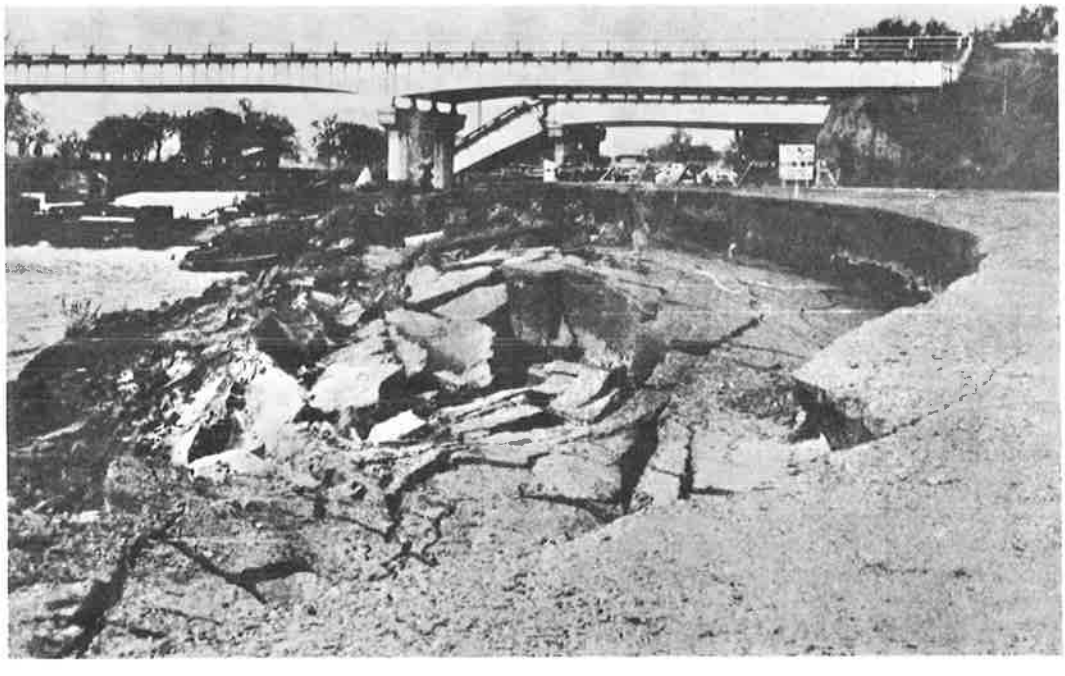

Figure 2. Subsidence of left bank following collapse of upstream I-29 bridge.

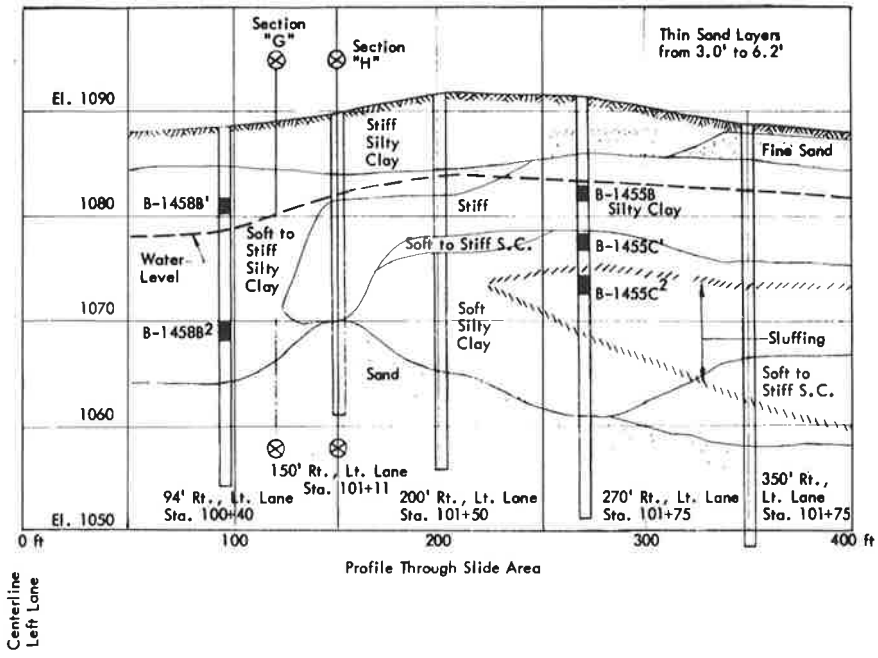

Figure 3. Soil profile through slide area south of bridge failure.

Immediately following the collapse of the bridge, pertinent data and related descriptions were collected by various agencies, including the Highway Departments of Iowa and South Dakota, the Bureau of Public Roads, and the Corps of Engineers. Much of the following information is based on reports and data relating to the hydraulics of the Big Sioux River collected by these agencies.

A secondary consequence of the conditions that caused the collapse of the bridge was the subsidence of the left bank just downstream of the highway spans and opposite the large scour hole that developed downstream of the structure. Figure 2 shows the area in which the subsidence occurred and the character of the settlement near the pier of the downstream bridge. Figure 3 shows the results of borings made in the left bank near where the subsidence occurred. The material labeled "soft silty clay" underlying the surface layer is significant. It might be concluded that the subsidence resulted from the removal of the lateral support of the left bank by the large hole eroded downstream of the bridge at the time of the collapse. The overburden then tended to squeeze the soft clay out into the river with the consequent subsidence of the bank itself. Some concern was felt at the time of reconstruction of the upstream bridge that the area of subsidence might be enlarged and endanger the nearby piers of the downstream bridge.

Hydraulically speaking, the essential characteristics of the replacement bridge were the increased span and the cylindrical piers that were used to support the bridge. The central span of the new bridge was such that the piers were essentially out of the channel itself, so that for ordinary flows there was relatively little obstruction to the passage of the water. Also, the flow past the cylindrical piers was independent of their orientation, and consequently the resistance or other effect of the piers on the flow pattern was the same for any direction of flow. To support the piers of the new bridge and to strengthen the piers of the remaining bridge, H piles were driven to a very considerable depth (to elevation 960-970 ft, respectively), certainly beyond any depth to which the river might reasonably be expected to scour. Upon completion of the bridge reconstruction and rehabilitation, the physical situation became one in which the two bridges located just upstream of a bend in the river consisted of the upstream bridge

supported on cylindrical piers 225 ft apart and a downstream bridge on webbed piers having a central span of 120 ft so that the two central piers were located in the channel. In addition, the piers of the downstream bridge were aligned normally to the centerline of the bridge and consequently were skewed by about 25 degrees to the direction of flow in the main channel. A third characteristic of the situation was the subsidence of the left bank immediately downstream of the downstream bridge.

HYDRAULIC FACTORS INFLUENCING UNDERMINING OF PIER

The collapse of the upstream I-29 bridge was apparently the outgrowth of a number of causative factors which combined to create conditions antagonistic to the continued existence of the bridges. If any one of these factors had been inoperative there is a possibility that the collapse would not have occurred, but with all of them influencing the hydraulics of the flow through the bridge openings the destruction of the bridge was the result. The failure was due to the undermining of one of the piers by erosion of the streambed. The depth and extent of erosion depended upon the various factors in different ways.

Erosion or local scour is the consequence of a dynamic force created by flowing water upon a movable or erodible boundary or bed. Continuity states that the rate of erosion is equal to the difference between the rate of local transport and the rate of supply to the area. Symbolically this can be written as

$$\frac{d\,f(B)}{dt} = g(B) - g(s) \tag{1}$$

where f(B) represents the local bed elevation, g(B) is the rate of transport from the scoured area, and g(s) is the rate of supply into the scoured area. This expression can be used to describe many situations, including local scour. It states that when the rate of supply is equal to the rate of transport the bed is stable. The rate of supply depends on upstream conditions and may be equal to zero as is the case immediately downstream of a reservoir. The transport rate from the area of scour depends on the local boundary shear, which in turn depends on the velocity near the bed and the flow pattern or boundary geometry. The transport rate also depends on the character and resistivity of the sediment composing the bed. The bed sediment, whether it is cohesive or noncohesive, can be characterized by a critical boundary shear. If this critical shear is exceeded the sediment will move. At the same time the boundary shear acting on the bed will tend to decrease as the depth of scour increases because of changes in the flow pattern. The relative scour, and hence the undermining of the pier, then depends primarily upon the local velocity, the properties of the bed sediment, and the geometry of the system.

Discharge

The first unusual factor involved in the collapse was the flood discharge, which was larger than any previously recorded for the Big Sioux River. The maximum discharge at Akron, Iowa, the USGS Gaging Station, was 54,200 cfs. The previous peak discharge was 49,500 cfs in 1960. Previously the maximum discharge, which occurred in 1952, was only 33,000 cfs so that the flood of 1962 was 1.64 times as large as the maximum recorded discharge prior to 1960 and at the time of the original design. The frequency distribution of annual floods based on the records prior to the design of the bridge indicated that the 50-yr flood was about 42,000 cfs. This was approximately the discharge for which the bridge was designed. The frequency distribution based upon all of the records up to and including the 1962 flood is plotted in Figure 4, showing a distinct upward curvature as the maximum floods are plotted in relation to the previous record. These results suggest that the 1960 and 1962 peak discharges represent floods of a much longer return period than might be expected from the present record. It is also conceivable although extremely doubtful that some pronounced change may have taken place in the Big Sioux watershed so that the magnitude of the annual floods is now considerably greater than in the past.

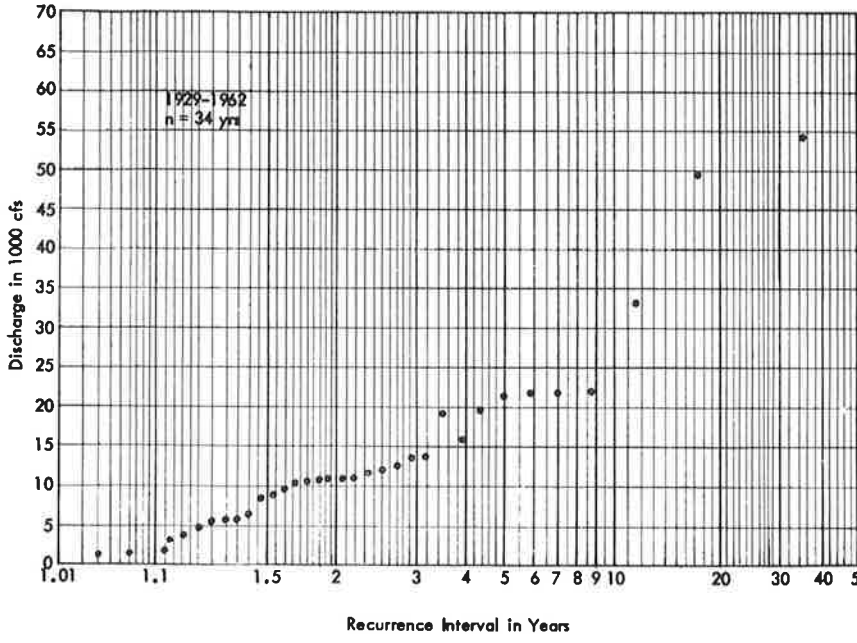

Figure 4. Flood-frequency curve for Big Sioux River at Akron, Iowa, 1929-1962.

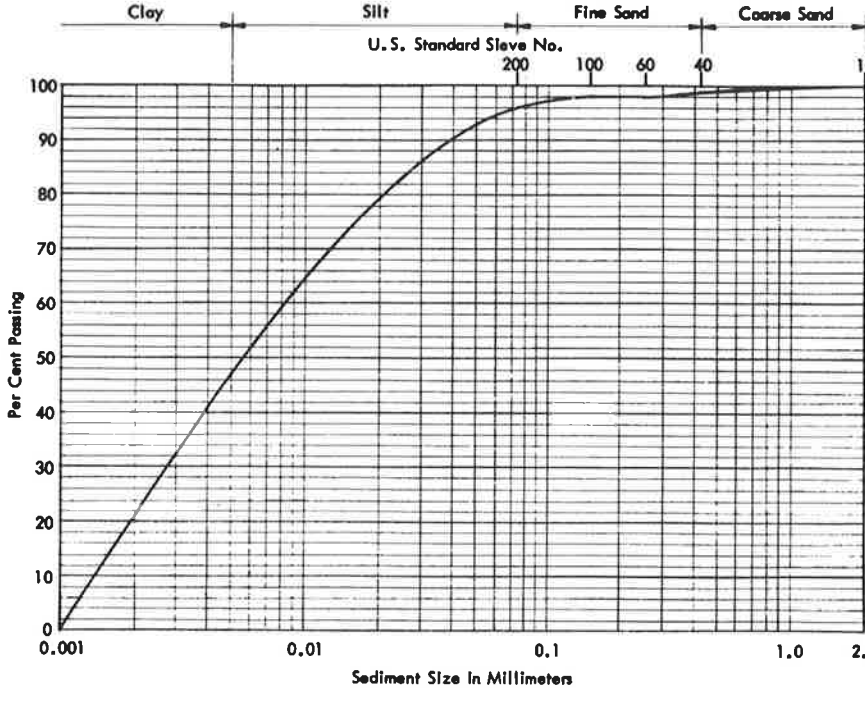

Mat'l. Pass. No. 40			Class Name	P.R.A. Class	Color
L.L.L.	L.P.L.	P.I.	Clay	A-7-6(19)	Grayish Brown
57	27	30			

Figure 5. Size analysis of composite sample of Big Sioux bed sediment.

The role played by the flood discharge is that of increasing the velocity in the river as a whole and particularly in the constricted section caused by the bridges. The increase in mean velocity of the stream can be seen from a flow equation such as the Manning formula

$$V = \frac{1.49}{n} R^{2/3} s^{1/2} \tag{2}$$

where V is the mean velocity, n is the roughness coefficient, R is the hydraulic radius, and s is the slope. Even if the slope remains constant the velocity will increase because of the increased hydraulic radius resulting from the enlarged cross-sectional area of flow. In addition a further increase in velocity approximately proportional to the discharge will result if the flow section is constricted, as at the bridge cross-sections. It follows then that the local velocity tending to cause scour around the bridge piers increases with the magnitude of the flood discharge.

Composition of Bed Sediment

The second factor involved in the local scour is the character of the bed sediment. In the Big Sioux River, it consists of material approximately 50 percent clay and 50 percent silt. The distribution curve of this material as obtained from a composite sample is shown in Figure 5. That the bed sediment of this composition is in a natural stream suggests very strongly that it possesses a high degree of cohesiveness and that the clay acts as a binder for the coarser particles. This implies that the resistivity of the bed to erosion depends primarily on the strength of the cohesive bond rather than the properties of the individual particles. While for noncohesive sediment the critical boundary shear at which movement begins depends primarily on the properties of the individual particles (size, shape, and density); for cohesive sediment the influence of size and other properties on the critical shear is masked by the greater bond strength. As a consequence greater force is necessary to erode initially the particles of a cohesive bed than for equivalent noncohesive beds, but once the bond has been broken the subsequent behavior of the bed particles in the flow depends on the particle properties only.

When shear forces are large enough to erode cohesive material, they are also large enough to carry the individual particles immediately into suspension and transport them through the section as part of the water complex. This suggests that for cohesive sediments there is relatively little material transported near the bed as bed load and that the rate of supply—g(s) in Eq. 1—into the cross-section where the bridges are located approaches zero. This means that the rate of scour depends only on the rate at which sediment can be transported from the scour hole and that the erosion will stop and the bed will become stable when the rate of transport out of the scour hole approaches zero. This will happen when the gradually decreasing boundary shear has been reduced to the critical shear for the bed material in the scour hole. It is clear then that size and depth of the hole will depend on the strength of the cohesive bond. One expects therefore that if the sediment of the riverbed had been noncohesive so that bed transport could have occurred, the local depth of scour at the obstruction would have been somewhat less than that actually generated.

Control of Stages on Missouri River

Before completion of the control structures on the Missouri River, the stages of the Missouri were the consequence of the normal runoff from the watershed basin. These stages more or less coincided with the flood stages of the tributary streams and a relatively high stage of the Missouri created backwater stages on the tributary streams. Thus the depths in the tributaries were greater but the slopes were much smaller so that high stages on the main stem reduced the flood velocities and hence the erosion potential. With the completion of the reservoirs on the Missouri, the stage at any point, and particularly those points downstream of the system of reservoirs, was de-

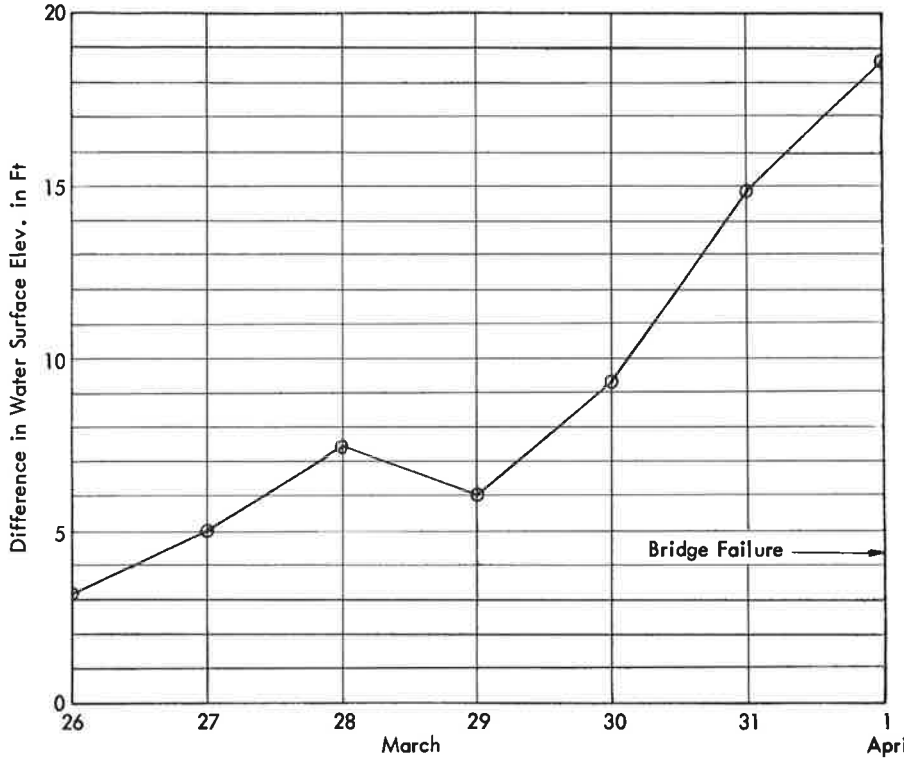

Figure 6. Difference in water surface elevations between Highway 77 bridge at Big Sioux River and combination bridge of Missouri River at Sioux City for week preceding bridge failure.

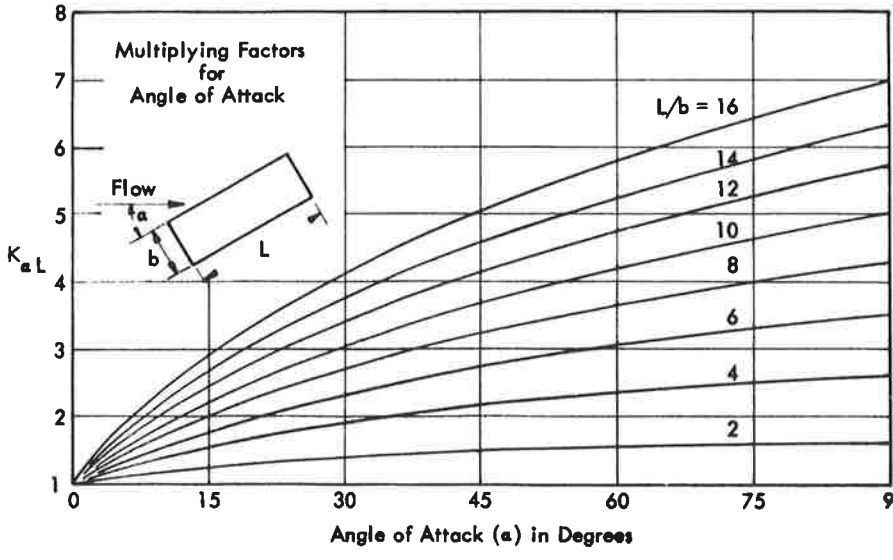

Figure 7. Design factors for piers not aligned with flow.

pendent on the artificial release of water from the upstream reservoirs and thus was relatively independent of the stages of the smaller tributaries during the flood season. In the case of the Big Sioux River during the 1962 flood at Sioux City the difference in elevation between gaging stations on the Big Sioux and on the Missouri increased from about 3.2 ft on March 26, 1962, to 18.6 ft on April 1, 1962 (Fig. 6). In this particular instance the stage of the Missouri remained relatively constant while that of the Big Sioux during the course of the flood increased very appreciably.

The consequence of the increased gradient or surface slope is a higher velocity than would be the case with a smaller slope. Visual observations of the flow in the Big Sioux shortly after the collapse of the upstream bridge indicated a velocity in the neighborhood of 13 ft/sec and, although the flood exceeded the design flood by a considerable amount, the stage at the bridge was still below that for which the bridge was designed. The high velocity resulting from the low stage of the Missouri tended to increase the shearing or erosive forces on the bed of the Big Sioux beyond that normally expected and hence subjected the bridge area to larger scouring forces.

Geometry of Piers

A fourth factor involved was the geometry of the piers supporting the bridges of the Big Sioux crossing. These piers consisted of two main columns with an intervening web to form a unified structure. Two of the piers of each bridge were founded in the river and constituted an appreciable obstruction and constriction to the flow. In addition the piers were constructed at right angles to the bridge centerline which was considerably skewed to the direction of flow. The angle of attack of the bridge piers to the mean flow was approximately 25 degrees.

Research on the erosion around bridge piers (1) has shown that the angle at which a pier is aligned to the flow is very significant in the extent of erosion that takes place around it. The two factors involved are the angle of attack and the length-breadth ratio of the pier. These results are shown in Figure 7 (1). Thus for an L/b ratio of 10 and an angle of attack of 30 deg, one could expect about three times as much scour as would occur if the pier had been aligned to the flow. For a cylinder in which the L/b ratio is unity, the multiplying factor is also unity since all orientations are equally favorable. Figure 7 clearly shows the importance of alignment of the piers in causing potential scour. It has been stated that the skewed alignment of the piers of the bridge was in anticipation of remedial work to be done on the Big Sioux River in which the reach through the bridges would be straightened by changing the location of the confluence of the Big Sioux with the Missouri River. If this change had been made, the degree of skewness or the angle of attack of the flow would have been considerably reduced.

The several factors affecting the stability of the bridge which have been enumerated are not, in general, subject to modification except perhaps the alignment and spacing of the piers. Aside from these factors it appears that an unfortunate combination of conditions led to the erosion. The value of analysis and of the availability of sufficient data lies in making provisions in the design for such contingencies.

The upstream bridge was reconstructed with cylindrical piers spaced 225 ft apart so that the flow obstruction was greatly reduced. The downstream bridge was strengthened by underpinning. For both bridges additional H piles were driven to provide ample support for the piers from further scour. In addition riprap and timber piles were placed on the left bank to prevent further subsidence of the bank and to protect the piers of the downstream bridge.

THE MODEL AND ITS VERIFICATION

To test the adequacy of these works in relation to their influence on the flow pattern, a model study was conducted at the St. Anthony Falls Hydraulic Laboratory. The studies were performed in an undistorted 1:75 scale movable bed model. The reach covered by the model consisted of a length of approximately one-half mile upstream and downstream of the bridges, and incorporated the bend just downstream of the bridges. Figure 8 is a general view of a portion of the model showing the bend. The banks of the model stream with the exception of the region near the bridges were made

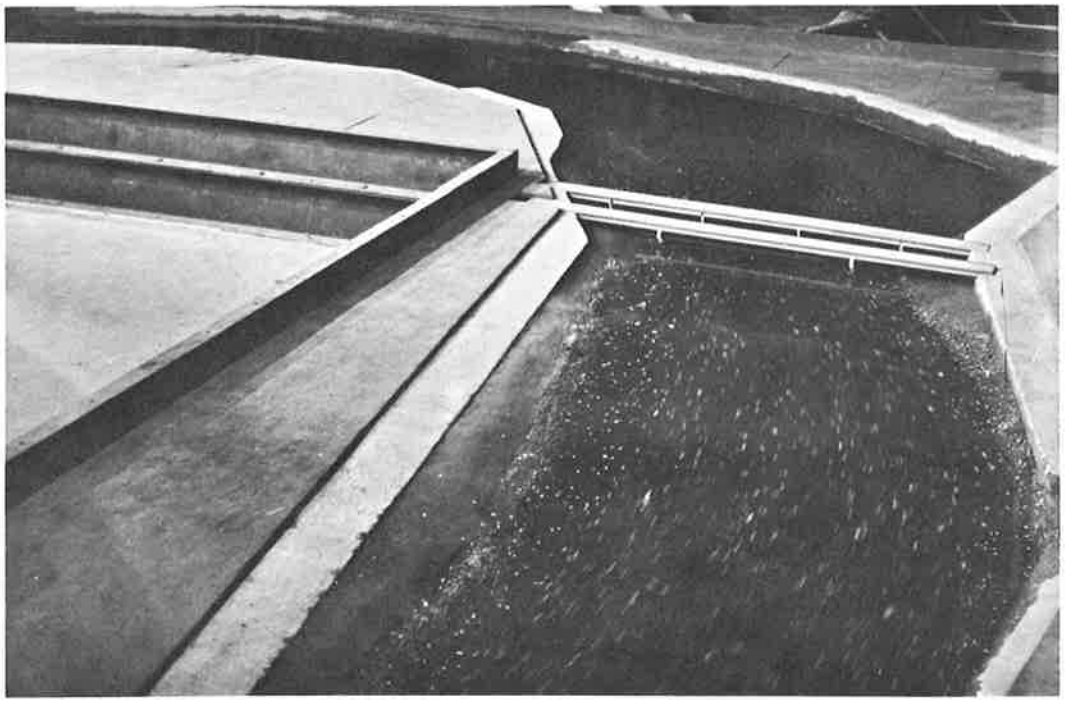

Figure 8. Overall view of Big Sioux model showing location of reconstructed bridges and the Big Sioux Bend downstream.

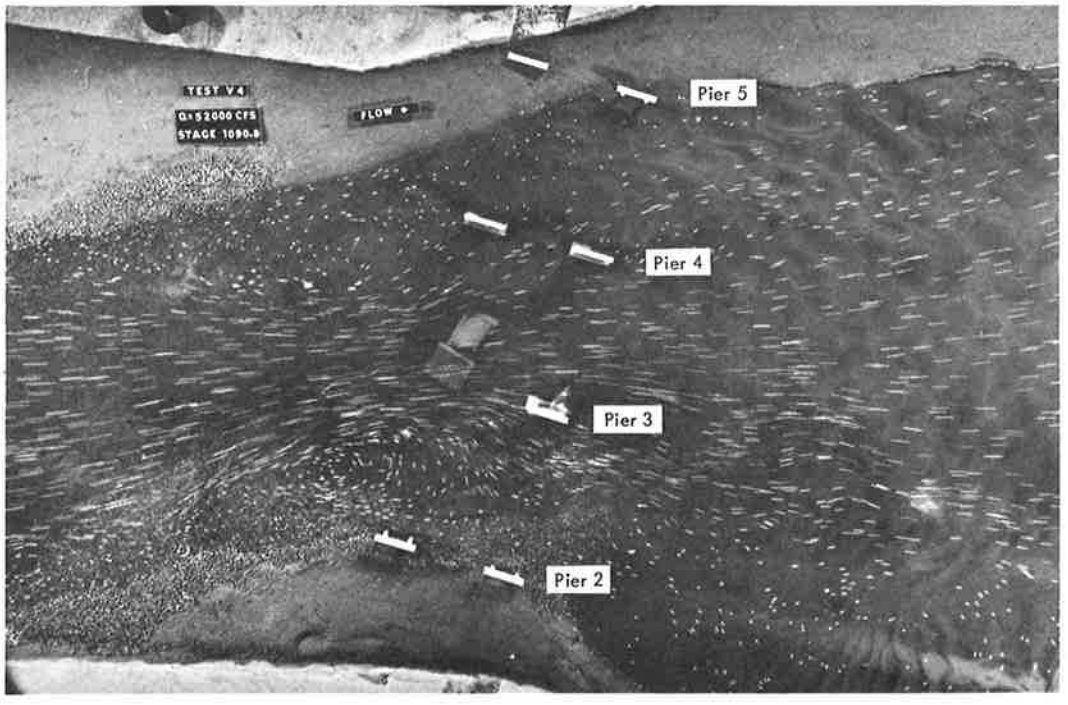

Figure 9. Verification test of hydraulic model showing collapse of pier 3 due to undermining; flow pattern delineated by confetti on water surface.

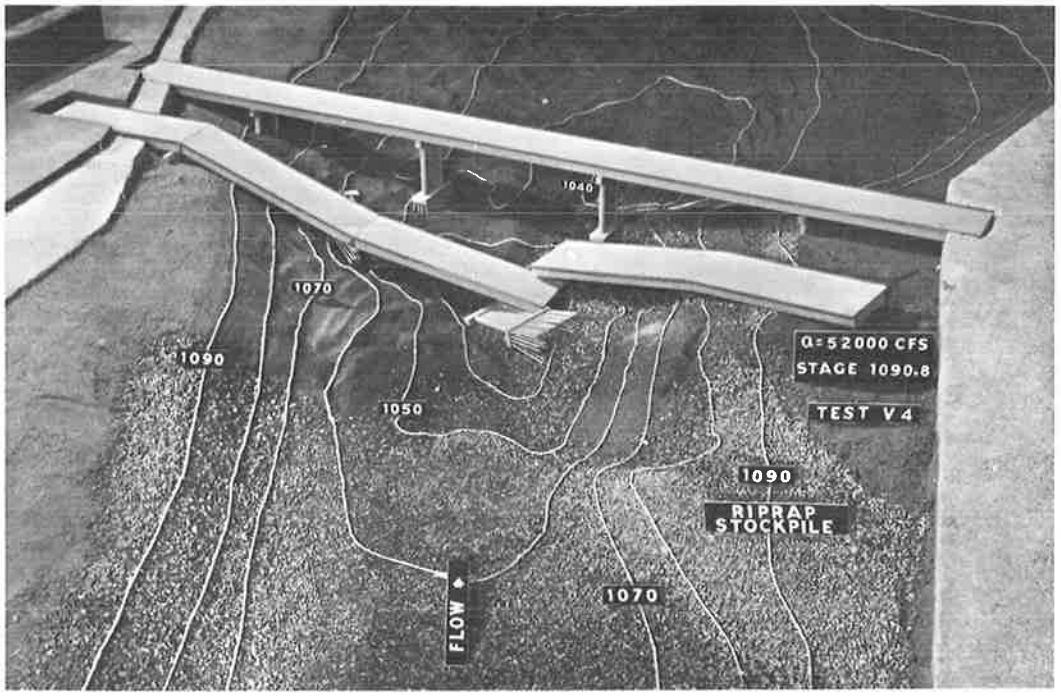

Figure 10. Erosion pattern following verification tests.

rigid so as to define the channel. The bed of the model consisted of a fine sand approximately 0.2 mm in size (initially, no attempt was made to simulate the cohesiveness of the upstream bed). The bridge piers were constructed to scale with the piles under the piers also made to scale.

In situations involving local scour the observed scour geometry is the result of the action of two types of forces. The flow of the water is a gravitational phenomenon while the removal of sediment from the scour hole depends on the size of the sediment and on the bed shear forces generated by the flow. These are complex functions of the viscous properties of the fluid. Generally it is not possible to satisfy exactly these two conditions at the same time in a small-scale model. In practice the model is designed and operated according to the gravitational requirements (Froude law) with the size of the model sediment adjusted so that qualitatively similar scour patterns will be developed. Because of the uncertainty introduced by the combination of two or more of these criteria recourse is had to the so-called verification process, wherein the model is operated as dictated by the gravitational requirements and then successively adjusted until it duplicates some significant observed event in nature. When this verification has been achieved so that qualitatively, and sometimes quantitatively, similar scour patterns are developed, it is assumed that the model will also simulate the scour pattern generated by a modification of the flow geometry.

The initial verification tests in the model were designed to determine its ability to simulate the conditions in the prototype that existed prior to the failure in order to duplicate the failure as it occurred in nature. The initial tests were made with the original piers with the model subjected to a flow corresponding to the 1962 flood. Initially, however, the model pier was not undermined as it should have been. The reason was that the bed of the model consisted of a noncohesive movable sand which as it was transported down the channel served to replace that which was removed around the pier so that the depth of scour was diminished and the system reached an equilibrium at a stage such that failure would not occur. It was therefore necessary to simulate the cohesiveness of the upstream bed material so that it would not contribute to the bed

transport. Since the cohesive sediment in the prototype would have gone into suspension upon the rupture of the cohesive bond, it would have played no part in the stability of the structure.

This result could be duplicated by preventing the erosion of the material upstream of the bridge. This was done by placing a thin layer of gravel on the bed upstream of the structure. This fine gravel was of such a size that it would not be moved during the flood. No gravel was placed in the region around the piers so that local erosion could occur and the bed regime could then correspond to that which was found in nature. By doing this, it was possible to duplicate the failure of the upstream bridge through the collapse of pier 3 and the creation of a large and deep scour hole downstream of the bridges. The flow pattern and the submerged pier for the verification test are shown in Figure 9, and the erosion pattern resulting from the flow is shown in Figure 10. After the pier collapsed the bridge spans were put in place in order to develop the final scour pattern as it occurred in nature (Fig. 10). The simulation of the conditions for the failure of the upstream bridge represented the verification of the model, and it was assumed that new patterns observed in the model would correspond to those in the prototype for the same conditions.

TESTS OF PROPOSAL FOR STABILIZATION OF LEFT BANK

On completion of the verification tests and before modification of the model was undertaken to incorporate the initial corrective measures, additional study by the Iowa State Highway Commission of the stability of the left bank resulted in a revised proposal. (It should be borne in mind that two problems existed at the bridge site: one was the safety of the bridges from undermining and the other was the stabilization of the left bank—the solution of the second problem insofar as riprap and other revetment

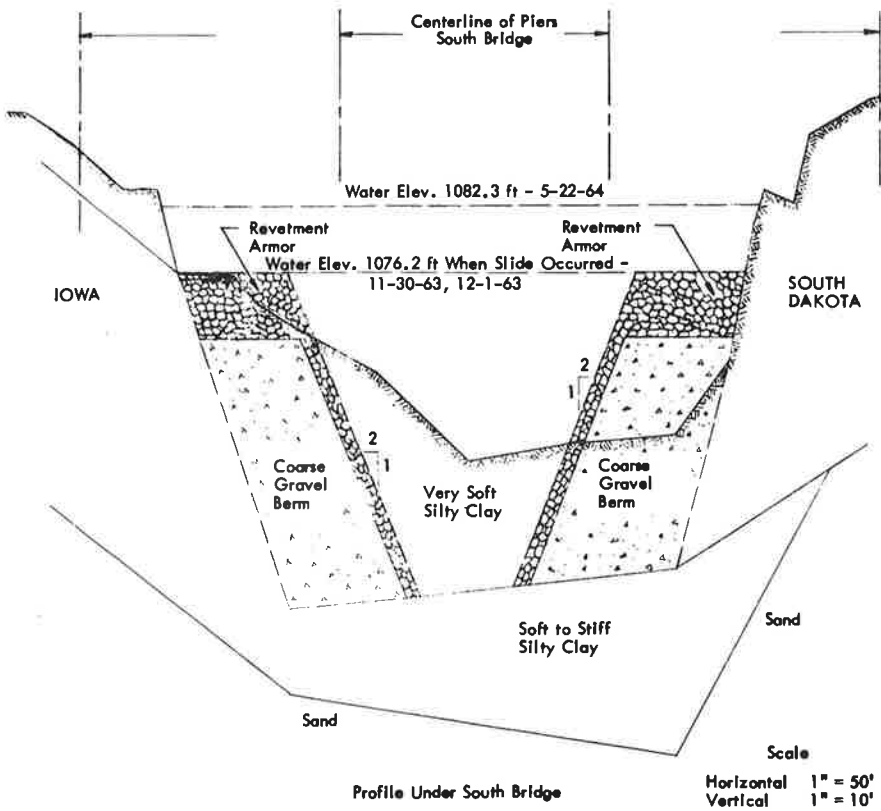

Figure 11. Stabilization proposal of Big Sioux channel for I-29 bridges.

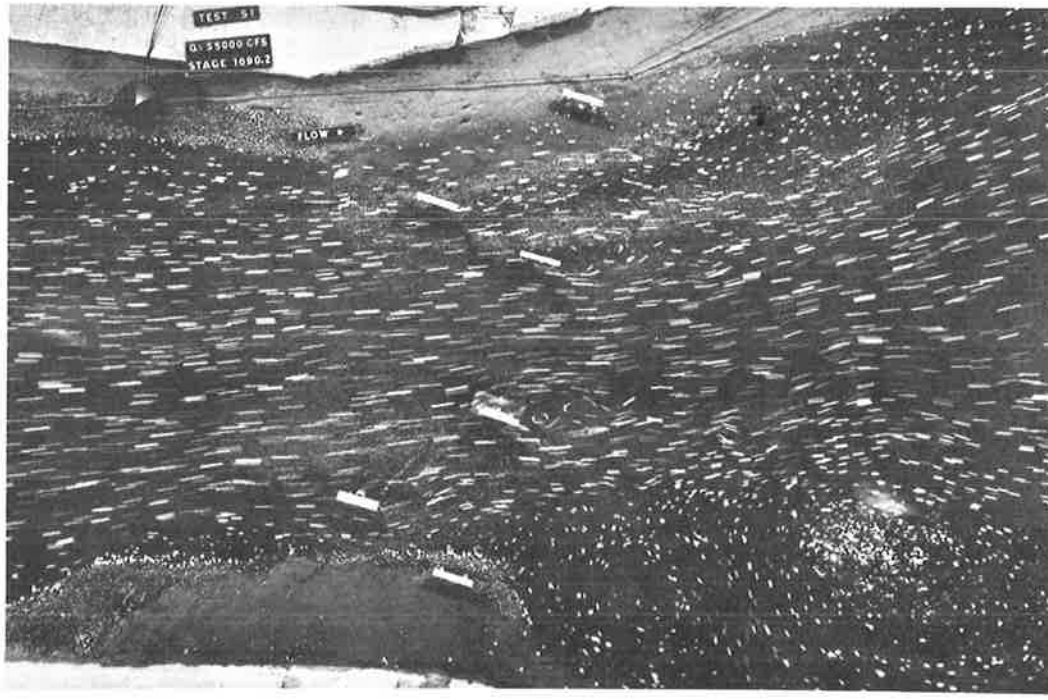

Figure 12. Flow pattern through bridge section with reconstructed bridges and with proposed berms and revetment in place.

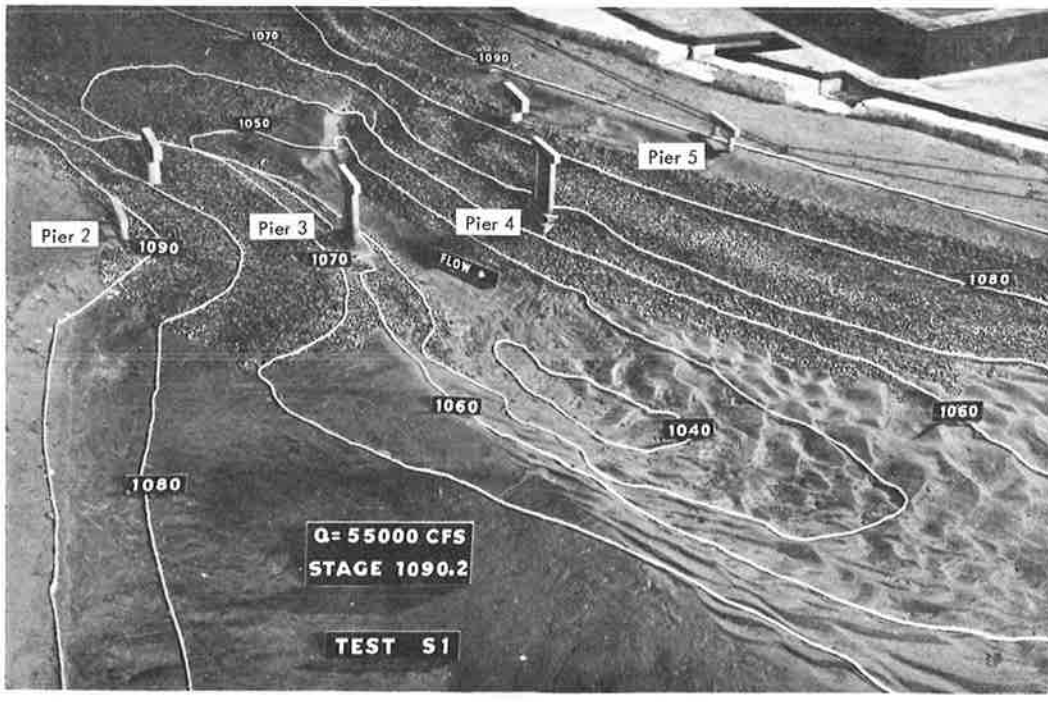

Figure 13. Erosion pattern resulting from flow through reconstructed bridges and protective works.

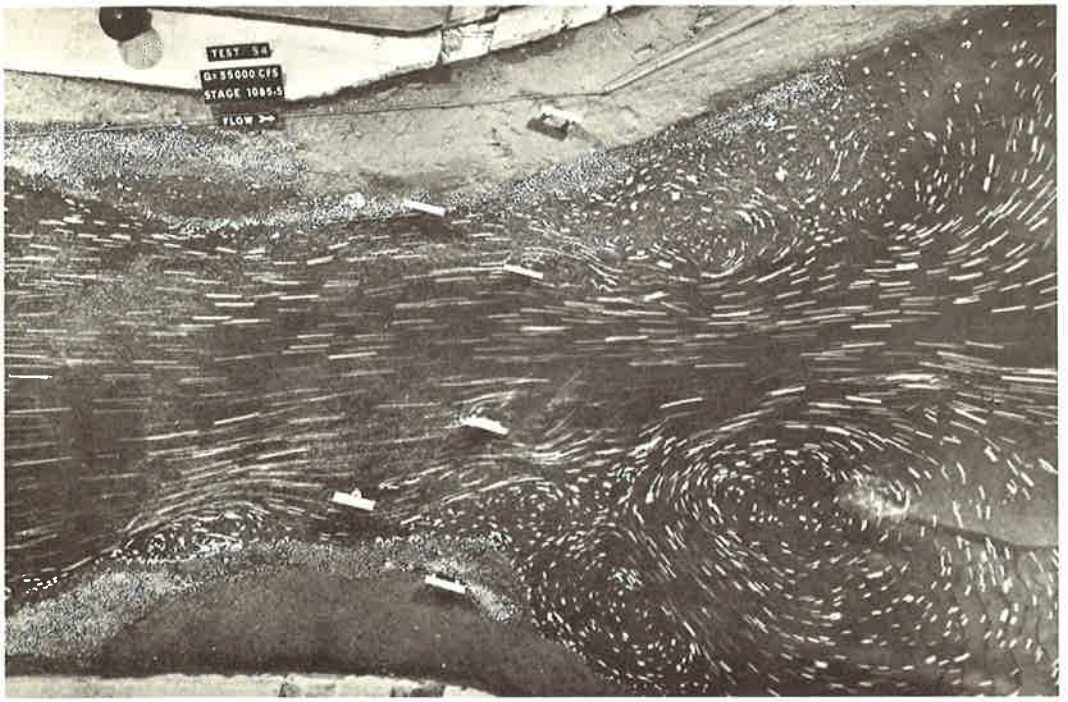

Figure 14. Flow pattern through bridge section with reconstructed bridges and proposed berms and revetment for maximum discharge simulating very low stage in Missouri River.

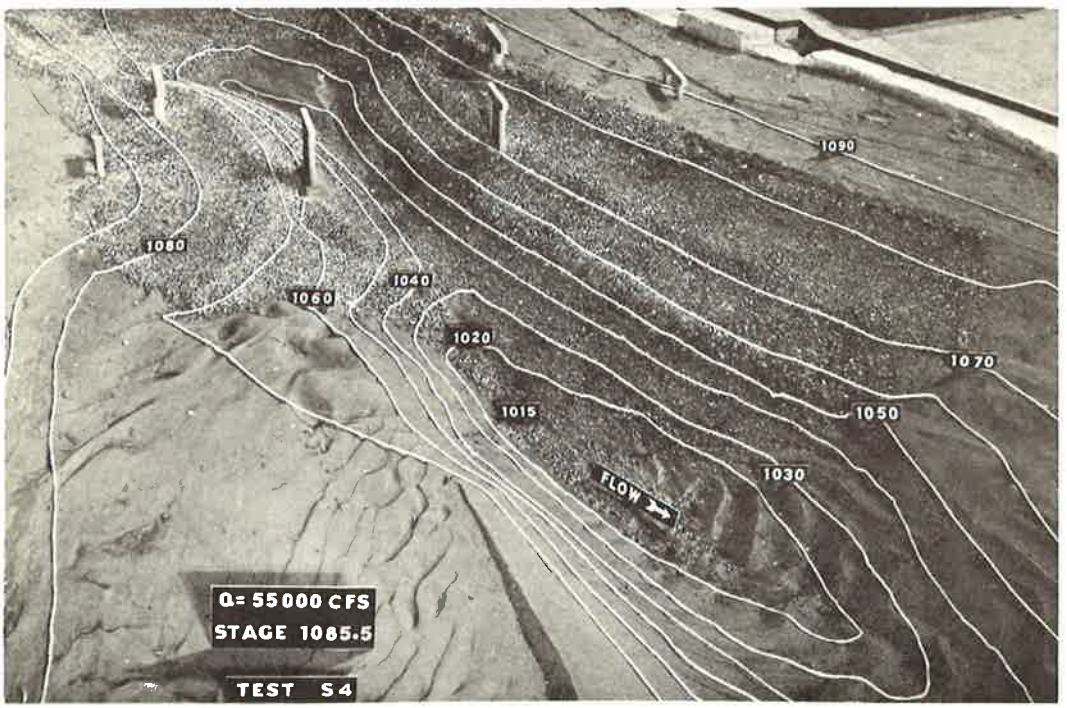

Figure 15. Erosion pattern resulting from maximum flow and low tailwater.

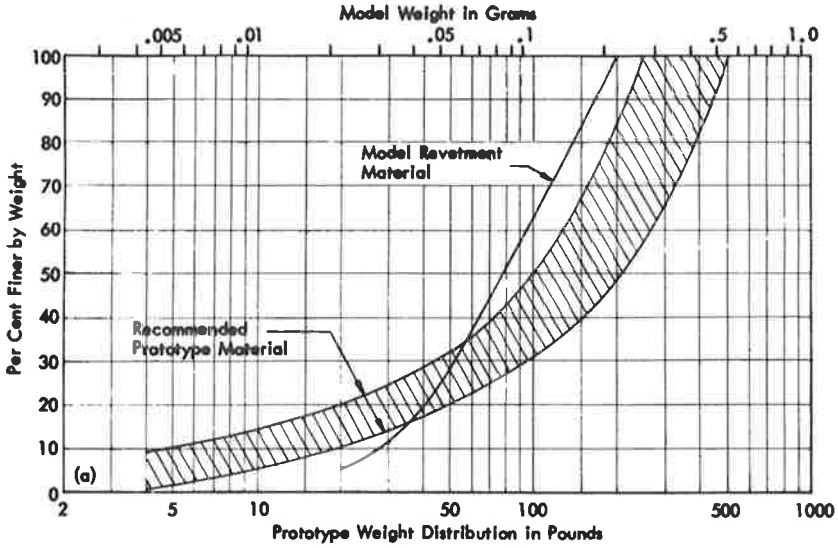

Figure 16. Revetment material weight distribution.

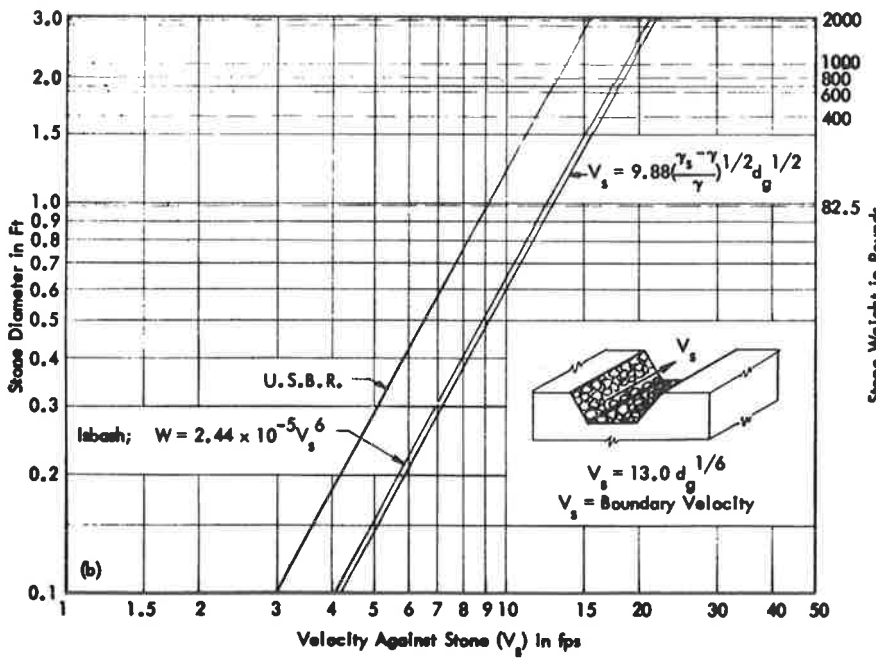

Figure 17. Critical velocities against stones.

was to be used might also constitute a solution for the first.) Stability studies indicated that the material required to stabilize the bank would have to be much more extensive than that previously proposed. Based upon this study the highway department proposed the plan shown in Figure 11. It consisted of rather extensive, coarse gravel berms protected by riprap revetment. These berms and revetment were to be placed on both sides of the river at the bridge cross-sections and extend downstream on the left

bank to encompass completely the area of subsidence. It was apparent that the berms and revetment would appreciably encroach upon the waterway area, although the depth to which it was proposed to carry the protective works was considerably below the original stream bed elevation.

If the necessity of the bank stabilization is accepted, the hydraulic problem then becomes one of determining the influence of the proposed protective measures on the flow and the effect of the flow upon the berms. Since the proposed berms and revetment also encompassed the two central piers of the downstream bridge, the problem of undermining the pier was no longer relevant as long as the proposed riprap could not be moved by the flood flows.

The model was modified to incorporate the proposed berms and revetment, the new piers for the upstream bridge, and the additional pile underpinning of the downstream bridge. Tests were made at a discharge of 55,000 cfs and were adjusted so that the stage at the bridges would be the same as that measured during the 1962 flood. The flow pattern that developed for these conditions is shown in Figure 12. The streaks on the surface are the images of confetti particles recorded over the exposure period. The elapsed time is recorded by the motion of a white streak on the disk revolving at a rate of one revolution per second. The elapsed time in this case was about $\frac{1}{5}$ sec. The photograph also clearly delineates the wake downstream of the skewed piers of the downstream bridge and the large clockwise whirl that developed at the outside of the bend downstream of the bridges.

One measure of the influence of the proposed corrective works is the increase or decrease in upstream stage as compared to conditions without the changes. One of the questions that was raised was the possibility of increased flooding upstream. Observations in the model showed that the stage was actually lowered after the stabilizing berms had been installed; the reason for this is shown in Figure 13, which shows the erosion pattern caused by the flow illustrated in Figure 12. The central portion of the channel that is unprotected by riprap has been eroded to enlarge the flow section, but the riprap protecting the banks and the piers has not been disturbed. The depth of scour downstream of the piers should be noted. Scour of this magnitude and location was observed in the prototype. In this case, however, the excessive scour in this area appears to be due to the action of a relatively high velocity jet through the bridge piers impinging upon the unprotected bed downstream. In this study it was assumed that the riprap to be used in the prototype would be of such a size that it would not be moved by the flow. The size required cannot be established by the model experiments but must be determined by other means. Given that the revetment would not be moved, the model revetment was chosen so it also would not be moved by the model flow. As a consequence of this, the flow pattern generated in the model would be similar to that generated in the prototype, and so also the scour pattern developed in the model will be at least qualitatively similar to that which would be developed in the prototype.

These results were the outcome of experiments in which the stage at the bridges was maintained at a level corresponding to the stage measured in the prototype. It appeared desirable to observe the effect on the bridge protection of a still lower stage as would be the case if the stage of the Missouri were artificially lowered. Such conditions are shown in Figures 14 and 15. Figure 14 shows the flow pattern for a discharge of 55,000 cfs when the stage at the bridge has been reduced to elevation 1085.5 ft. The separation zones are more distinct and the strength of the downstream whirl has increased. The jet effect caused by the piers of the downstream bridge is clearly shown as well as the high velocities initiating vortices at the inside bank of the bend. The erosion pattern created by this flow is shown in Figure 15. For these extreme conditions some of the riprap has raveled into the channel between the piers and in a downstream direction. The jet (Fig. 14) has eroded an excessively deep hole downstream of the piers. In spite of this, however, the piers themselves appear to be unaffected by the flow.

The effectiveness of the riprap revetment in protecting the piers depends on its ability to resist the dynamic forces generated by the flow. Experiment and experience have established a relationship between the velocity near the boundary and the size of the riprap necessary to resist movement. Figure 16 shows the size distribution curve of the model sediment transferred to prototype sizes. This material was stable in the

model. Using the graph in Figure 17 as a guide and considering the practical limits of quarry production, a recommended riprap size distribution is also shown in Figure 16 for comparison with the model riprap.

The hydraulic model studies of the flow pattern with the proposed gravel berms and riprap revetment indicate that the protection provided will be adequate for flood discharges considerably larger than those recently experienced if the field construction is similar to that tested in the model. The studies also serve to demonstrate the value of hydraulic model studies combined with analysis and field data as an adjunct to the design of bridges over waterways and other hydraulic structures.

ACKNOWLEDGMENTS

The cooperation in providing data and photographs and support for these model studies of C. A. Pestotnik of the Iowa State Highway Commision, P. H. Schultz of the South Dakota Department of Highways, and Roy Warner and R. E. Gibson of the Bureau of Public Roads is acknowledged. The expert assistance of A. L. Charbonneau of the St. Anthony Falls Hydraulic Laboratory in carrying out these experiments is appreciated.

REFERENCE

1. Laursen, E. M., and Toch, A. Scour Around Bridge Piers and Abutments. Iowa Highway Research Board Bull. No. 4, Iowa Institute of Hydraulic Research, May 1956.

The Design of Supercritical Flow Channel Junctions

CHARLES E. BEHLKE, Professor of Civil Engineering, Director, Institute of Water Resources, University of Alaska, and
HAROLD D. PRITCHETT, Associate Professor of Civil Engineering, Oregon State University

The purpose of the paper is to discuss the diagonal wave and pile-up problems which result from the intersection of two open channels, each carrying water at supercritical velocities. Methods are set forth for the determination of the height of wall pile-up which occurs under conditions of design flow and under the unbalanced conditions of flow in only one of the channels. For the determination of pile-up height for these conditions it is necessary to refer to laboratory curves which are included.

A channel junction design is suggested which has minimized the wave problem in laboratory experiments. The junction differs from the simple channel junction in two ways. The main channel is widened at the junction to accommodate the increased discharge contributed by the side channel, and a baffle, which is actually only an extension of the main channel wall, is extended downstream in front of the side channel. This baffle is recommended to be tapered at a slope equal to the greater of the Froude numbers in the main or side channels, divided by 50. Smaller rates of taper are acceptable, but more pronounced tapers result in pile-up problems on the channel sides. This type of junction results in almost no wave problem under design conditions of flow in both channels and it results in low pile-up depths for conditions of flow only in one channel or the other.

•SUPERCRITICAL, or high velocity, flow differs from subcritical flow primarily because supercritical flow does not exhibit backwater effects. Disturbances created in subcritical flow are felt both upstream and downstream from the point of origin of the disturbance. However, in the domain of supercritical flow, disturbances do not travel upstream but can only travel downstream. Hydraulic engineers familiar with supercritical flow are well aware of the diagonal waves which propagate and reflect back and forth across the channel downstream from disturbances such as changes in alignment, transition sections, channel contractions, and channel expansions.

It is only natural for the hydraulic engineer to expect diagonal wave difficulties at, and downstream from, the junction of two supercritically flowing channels. Figure 1 shows a laboratory example of the nature of the diagonal wave pattern, which results from supercritical flow channel junctions, and the resulting wall pile-up and downstream wave propagation. The purpose of the research reported in this paper is to better define the diagonal wave difficulties and pile-up problems so evident in Figure 1, and to find ways to reduce or eliminate these wave problems.

Paper sponsored by Committee on Surface Drainage of Highways and presented at the 45th Annual Meeting.

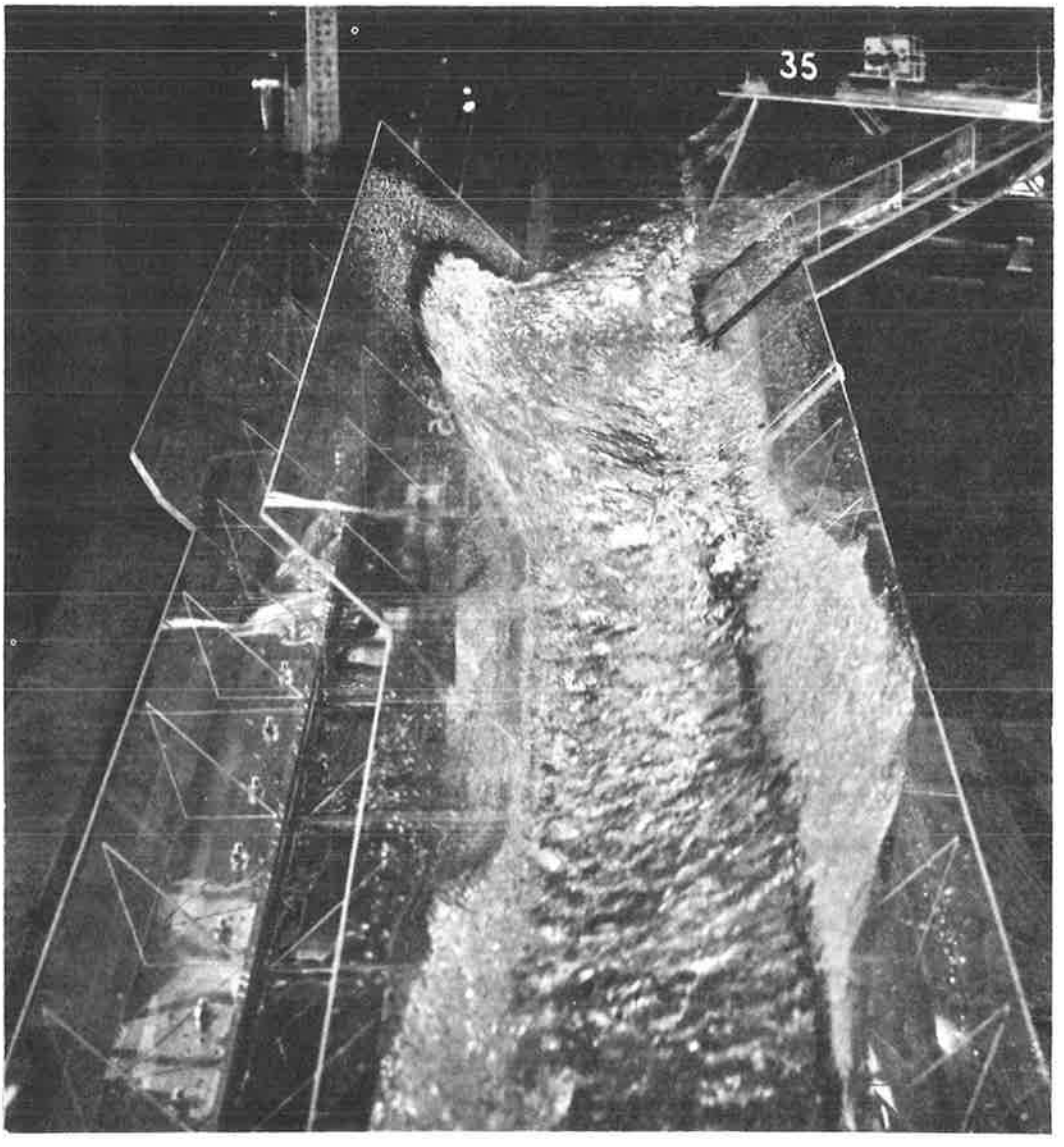

Figure 1. Wave problems created by a simple junction of supercritical flows in trapezoidal channels.

INTRODUCTION TO SUPERCRITICAL FLOW DISTURBANCE PHENOMENA

The following discussion is not intended to be comprehensive but is only intended to give the reader the necessary background to allow him to better understand the problems and the reasoning behind the solutions to the problems discussed in this paper.

The term "positive disturbance" will be applied to a disturbance which creates a wave of greater depth than that of the water feeding the wave. The type of positive disturbance which is most informative to consider is that shown in Figure 2. This type of phenomenon has been studied by Ippen (1), and by Ippen and Harleman (2). The factor which produces this disturbance is the channel's wall being deflected inward to-

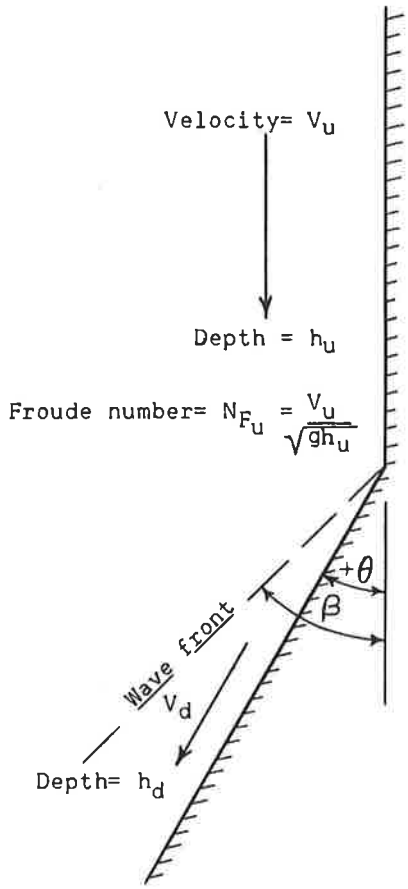

Figure 2. Effects of a simple, positive disturbance on supercritical flow.

ward the oncoming flow, resulting in a change in the direction of the velocity vector of the flowing water and an increase of depth. The velocity vector is deflected through the same angle as that of the wall deflection θ but the increase in depth occurs as the water passes through a diagonal wave which stands at an angle β to the projection of the original channel wall. The angle β is always greater than the angle θ. Though the wave is indicated as a sudden increase in depth, this wave is very abrupt for large values of β and may be quite gradual for small β values (2). The abrupt, vertical wave front (Fig. 2) simply forms a basis for discussion. Ippen has shown that the following equations relate the various parameters, defined in Figure 2, of this disturbance and the flow.

$$\sin \beta = \frac{1}{N_{F_u}} \sqrt{(1/2)\left(\frac{h_d}{h_u}\right)\left(1 + \frac{h_d}{h_u}\right)} \qquad (1)$$

and

$$\frac{h_d}{h_u} = \frac{\tan \beta}{\tan (\beta - \theta)} \qquad (2)$$

Simplification of these equations does not appear possible; however, they are presented in graphical form in Figure 3.

Depths of flow in the positive wave are often somewhat greater than the depth of flow in the region downstream from the wave.

An important aspect of positive disturbances is the resulting wave is transmitted in a straight line diagonally across the channel almost without change of shape. This wave can be directed as a concentrated disturbance in desired directions by controlling the wall angle θ. For a given Froude number, in the upstream zone, $N_{F_u} = V_u/(gh_u)^{1/2}$, however, the intensity h_d/h_u of the directed disturbance is determined by Eq. 2. So, for given upstream conditions, it is possible to change the direction of the diagonal wave by changing the wall angle θ but the disturbance intensity cannot be controlled independently of the wall angle.

The possibility of directing concentrated, positive disturbances at a desired point has great application in supercritical flow channel transitions from a wider to a narrower channel and in the area of open channel bends (1). This principle will be applied later in this paper.

A negative disturbance, in contrast to a positive disturbance, is created most simply by a change in channel wall alignment (Fig. 4). The wall deflection angle θ is negative, and the depth decreases downstream from the dashed line. However, the decrease in depth is sudden only at the break in the wall alignment.

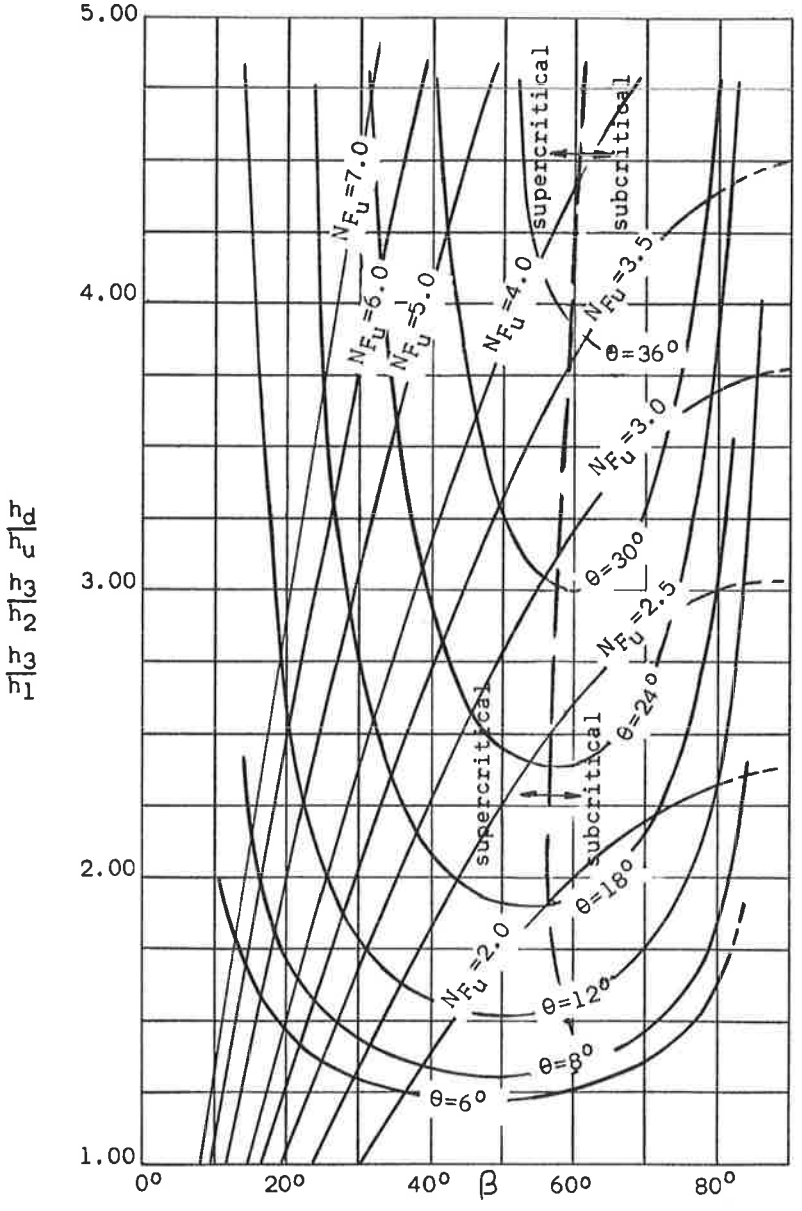

Figure 3. Plot showing relationships between θ, β, $h_{downstream}/h_{upstream}$, and upstream Froude number.

Farther out in the flow and farther downstream the change in depth is gradual. Rouse et al. (3) have investigated this at some length. The type of disturbance indicated in Figure 4 can result in a change in the direction of the velocity vector being more negative than the negative change in alignment of the wall. This can result in the creation of a positive reflection originating at some point along the wall downstream from the alignment change. This creation of a positive disturbance as a result of an upstream negative disturbance is one of the phenomena which works against the designer in many applications.

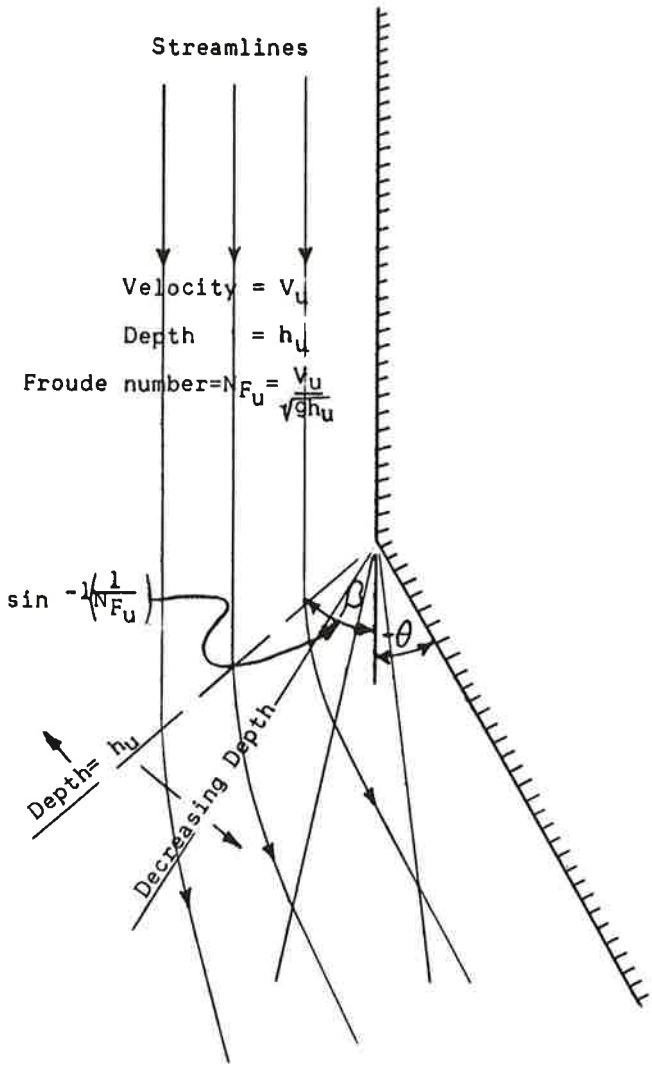

Figure 4. Effects of a simple negative disturbance on supercritical flow.

Probably the most important point to note about negative disturbances is that they are concentrated only at the point of origin, and they fan out from that point. It is not, therefore, possible to direct a negative disturbance in a concentrated form to some point away from its point of origin.

In the design of transitions, bends, and junctions, both negative and positive disturbances are created. Positive disturbances are usually directed at the point of origin of a negative disturbance in order to cancel the effects of both. However, attempts to direct a negative disturbance toward the point of origin of a positive disturbance result in only limited success.

THE LABORATORY APPARATUS

Because laboratory results will later be used in conjunction with the analysis to assist in design, and because the laboratory work paralleled and assisted in the determination of realistic assumptions to be made in the analysis, the discussion of the laboratory apparatus will precede the analysis.

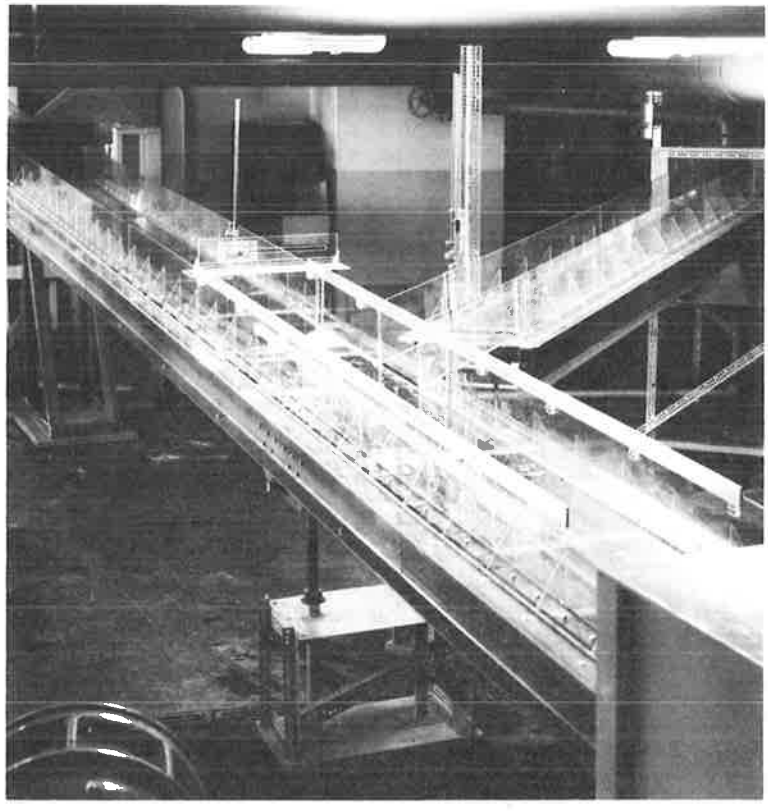

Figure 5. Laboratory channels and junction arranged for rectangular channels with a 45-deg angle of incidence.

The experiments were performed in the Oregon State University Hydraulics Laboratory. The laboratory apparatus, arranged for rectangular channel experiments, is shown in Figure 5. The main channel and the side channel were supplied with water from separate pumps. The main channel was 32 ft in length; its bottom width varied from 9 in. to a maximum of 18 in. for rectangular and trapezoidal channel experiments. The side channel varied from 18 to 22 ft in length, depending on the angle of incidence of the two channels; its width varied from a minimum of 6 in. to a maximum of 12 in. for the rectangular channel, and from a minimum bottom width of 6 in. to a maximum of 12 in. for the trapezoidal channel experiments. For the trapezoidal channel experiments the side slopes in both channels were 1:1. No attempt was made to consider other side slopes.

The slope of each of the channels could be varied independently. It was, thus, possible to vary the velocity and Froude number as well as the depth of flow in each channel independently.

The discrete angles of incidence α between the two channels were 15, 30, and 45 deg. It was felt that greater angles of incidence would be completely unrealistic.

Arbitrarily, the junction of the two channel inverts, for situations where the two channels combined with common invert elevations, was made along the line of intersection of the plane of the invert of the main channel with the plane of the side of the main channel. This required a warping of the sides and bottom of the side channel near the junction for all experiments. This was generally small, however, and did not greatly affect the depth of flow from side to side of the side channel at the point of juncture with the main channel.

Water was introduced from the laboratory piping system into box-type collectors from which the water entered the two channels. The flow distance between the upstream end of each channel and the junction appeared sufficient to create essentially uniform flow except as affected by the warping of the side channel in the vicinity of the junction.

Froude numbers for the flow in each of the channels varied from approximately 2 to approximately 7. Depths varied from 0 to approximately 0.2 ft. Velocities ranged up to approximately 10 ft/sec.

The discharge into the channels was measured by venturi and orifice meters. The depths of flow in the approaches to the junction were measured by piezometers in the bottom of each channel. Depths of flow in the disturbed sections and wall pile-up heights were measured with point gages from the top of the channel. The depth of flow in the side channel was measured just upstream from the entrance to the short warped section which terminated at the junction.

ANALYSIS AND LABORATORY RESULTS FOR SIMPLE JUNCTIONS

A diagram of a simple rectangular channel junction is shown in Figure 6. The term "simple" is applied here to mean that the two channels have common invert elevations and there are no baffles or piers of any kind to deflect the flows at the junction. Also, the main channel width is not increased downstream from a simple junction.

Figure 7 is a definition sketch of depths, Froude numbers, angles, etc., for flow conditions through a simple junction of rectangular channels.

Since the designer is usually faced with the problem of how much wall pile-up will occur and where it will occur for junctions of this type, the following discussion is aimed at a solution to this problem.

Observation indicates that the depth of flow immediately downstream from each of the diagonal jumps (Fig. 7) is the same. The depth of flow in this wedge-shaped zone is indicated as h_3, and the depths of flow in the main and side channels as h_1 and h_2. Since observation and intuition indicate that the two diagonal waves produce identical downstream depths, h_3, analysis of the problem is facilitated by the above assumption.

It should be observed that the energy level is not the same throughout the entire wedge-shaped wave area. The velocities in the main and side channels prior to the junction are probably not the same. This means that in the wedge-shaped zone the specific energy ($h + V^2/2g$) is different for water which had its origin in the main channel than for water which originated in the side channel. This difference in velocity may create an area of turbulent shear between the two velocity zones, extending diagonally across the channel in the wedge area (Fig. 8).

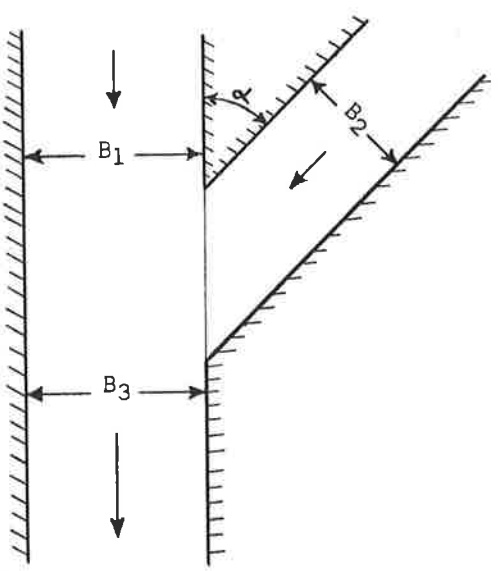

Figure 6. Plan view of simple junction of rectangular channels.

For analysis, it has been assumed that the effect of the side channel flow on the main channel flow is the same as the positive disturbance, wall effect previously described (Fig. 2). It is also assumed that the flow in the main channel has a similar effect on the flow in the side channel. The gravity effects of the channel slopes are neglected.

The wave angles β_1 and β_2 of Figure 7, can be determined, subject to the assumptions above, by combining Eqs. 1 and 2, written for each channel, with the facts that the value of h_3 is the same for the main channel water as it is for the side

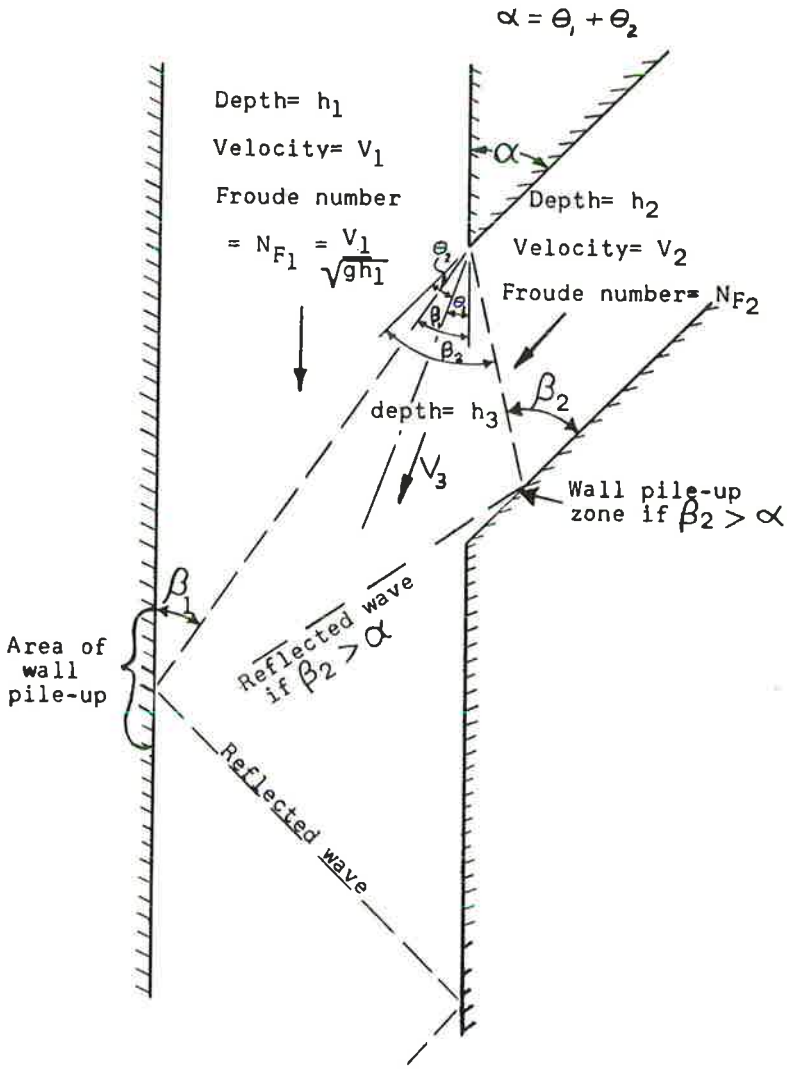

Figure 7. Definition sketch of a simple junction of rectangular channels.

channel and the sum of the two θ angles must equal the angle of incidence of the two channels. The equations are as follows:

$$\sin \beta_1 = \frac{1}{N_{F_1}} \sqrt{(1/2)\left(\frac{h_3}{h_1}\right)\left(1 + \frac{h_3}{h_1}\right)} \tag{3}$$

$$\sin \beta_2 = \frac{1}{N_{F_2}} \sqrt{(1/2)\left(\frac{h_3}{h_2}\right)\left(1 + \frac{h_3}{h_2}\right)} \tag{4}$$

$$\frac{h_3}{h_1} = \frac{\tan \beta_1}{\tan (\beta_1 - \theta_1)} \tag{5}$$

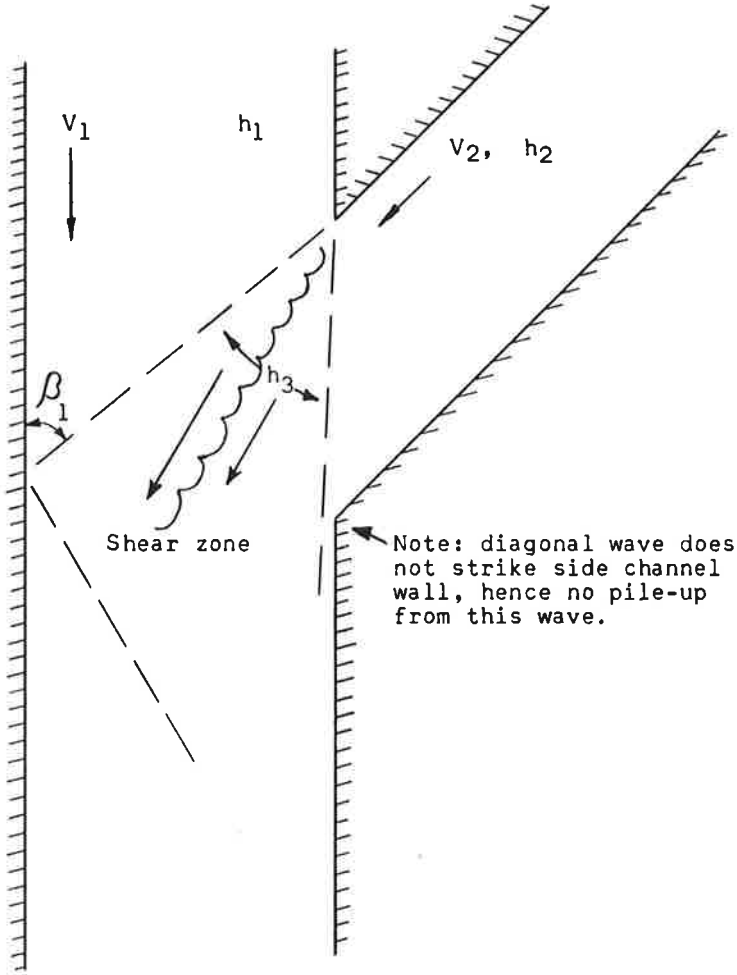

Figure 8. Shear zone between different velocity levels in the h_3 depth zone.

$$\frac{h_3}{h_2} = \frac{\tan \beta_2}{\tan (\beta_2 - \theta_2)} \tag{6}$$

$$\frac{h_3}{h_1} \div \frac{h_3}{h_2} = \frac{h_2}{h_1} \tag{7}$$

$$\theta_1 + \theta_2 = \alpha \tag{8}$$

It must be remembered that the designer would know the depths and velocities of approach for each of the channels and would know a proposed angle of incidence (which he may desire to change). The satisfaction of Eqs. 3 through 8 can be rapidly accomplished by trial and error use of Figure 3.

The wall pile-up which results from the reflection of the diagonal waves off the wall of the main channel or off the wall of the side channel is the thing of interest to the

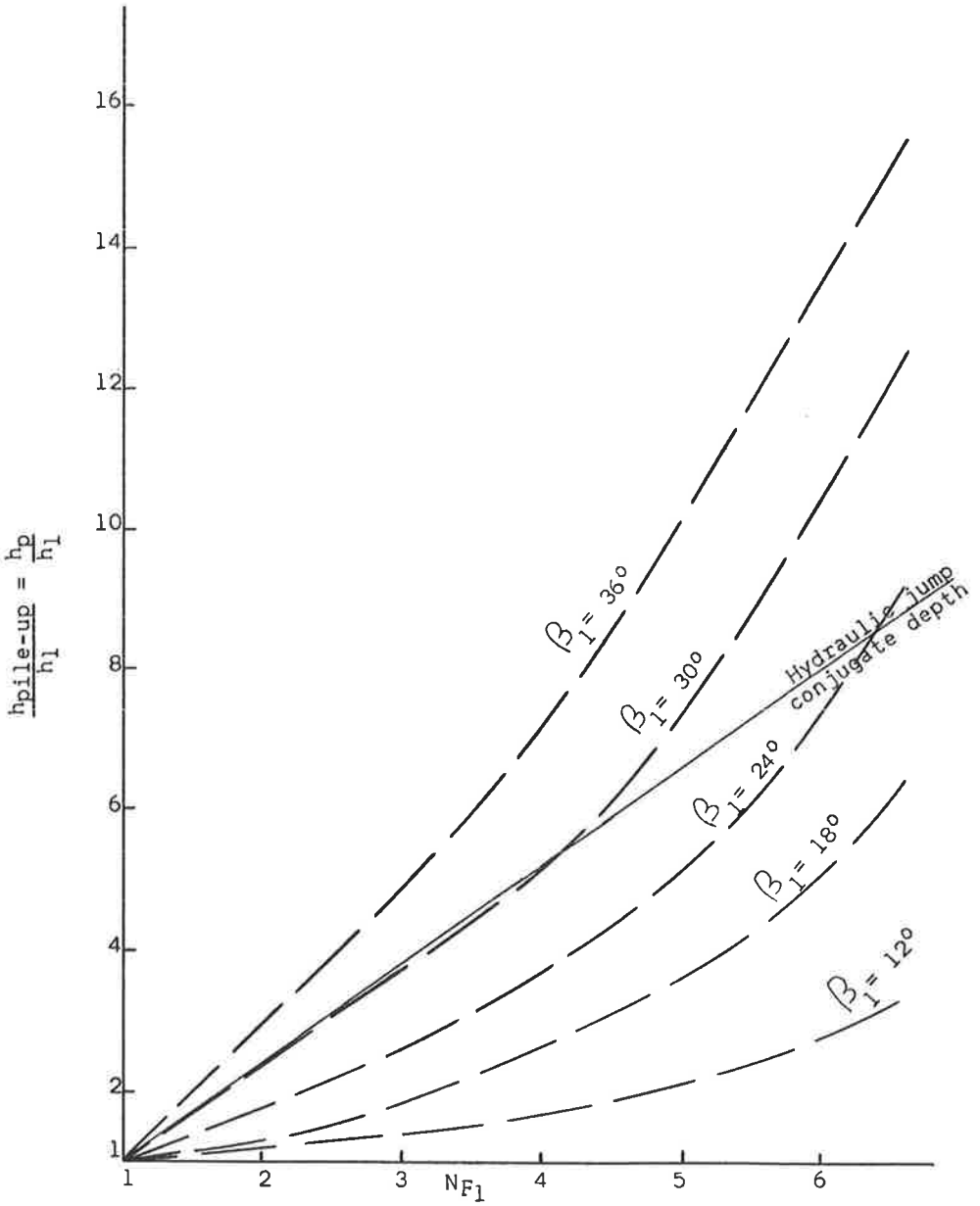

Figure 9. Experimental wall pile-up as a function of upstream depth and Froude number for $\beta_2 < \alpha$.

designer. However, the magnitude of the pile-up is a three-dimensional problem of analysis which has eluded the authors. The determination of the pile-up depth was, therefore, done in the laboratory. The results of the laboratory experiments for wall pile-up are given in Figure 9. The solid line indicates the depth which would result downstream from an ordinary hydraulic jump whose β angle is 90 deg. This is only shown to indicate the relative depths of pile-up possible.

It must be made clear that the plot of Figure 9 is only applicable under conditions where β_2 is less than α. If β_2 is greater than α, the diagonal wave of the side channel flow piles up on the side of the side channel and reflects out across the h_3 area. If it

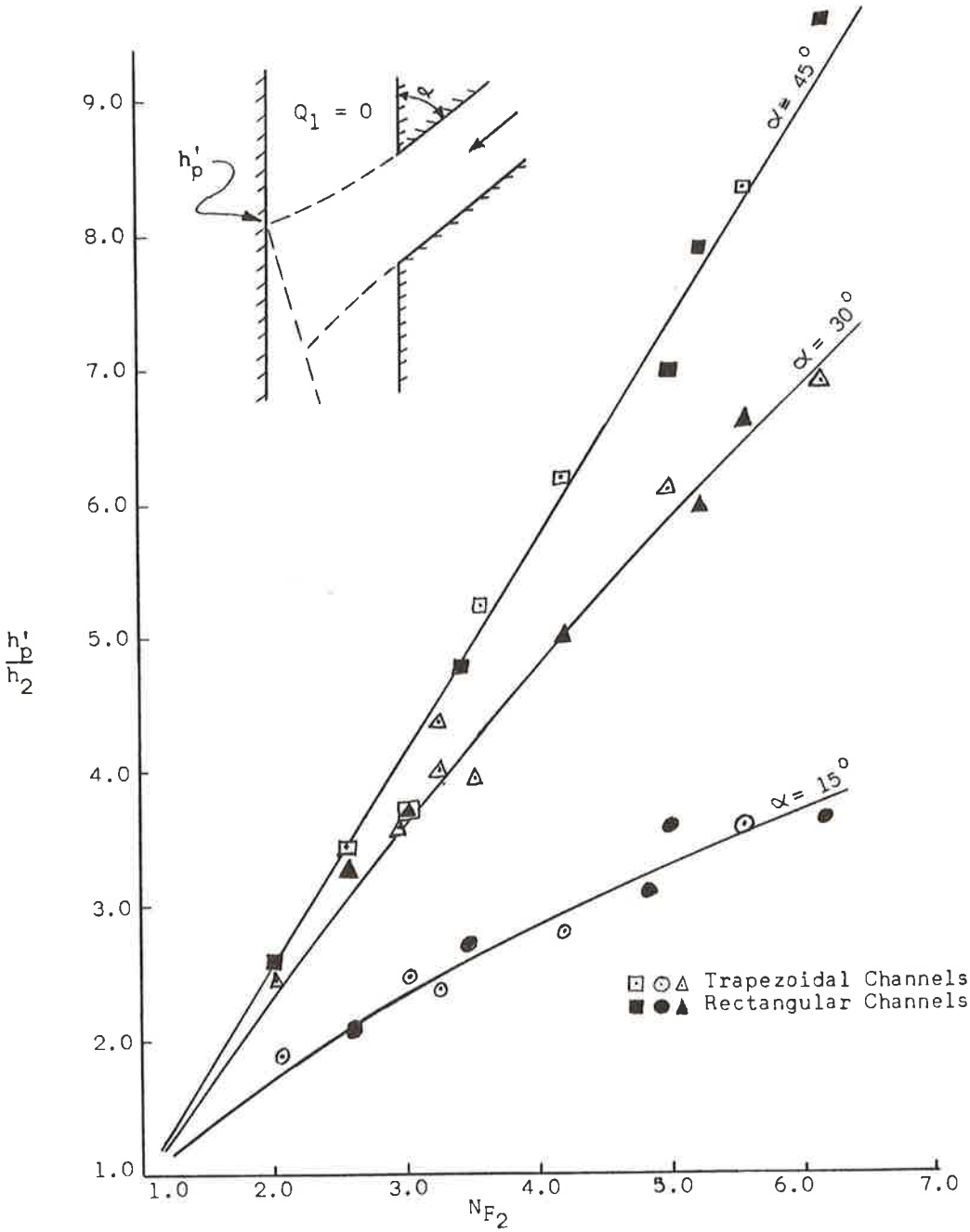

Figure 10. Relative pile-up on main channel wall resulting from flow in side channel only.

is found that β_2 is greater than α, the designer should make appropriate changes because it can be seen from Figure 9 that the pile-up on the wall of the side channel, indicated in Figure 7, can be quite appreciable for most values of $\beta_2 > \alpha$.

The best design of simple channel junctions is one in which β_2 just equals or is slightly smaller than α. This accomplishes the dual purpose of eliminating the pile-up problem in the side channel and it directs a positive wave at the beginning of a negative disturbance, thus eliminating the difficulties introduced by the negative disturbance.

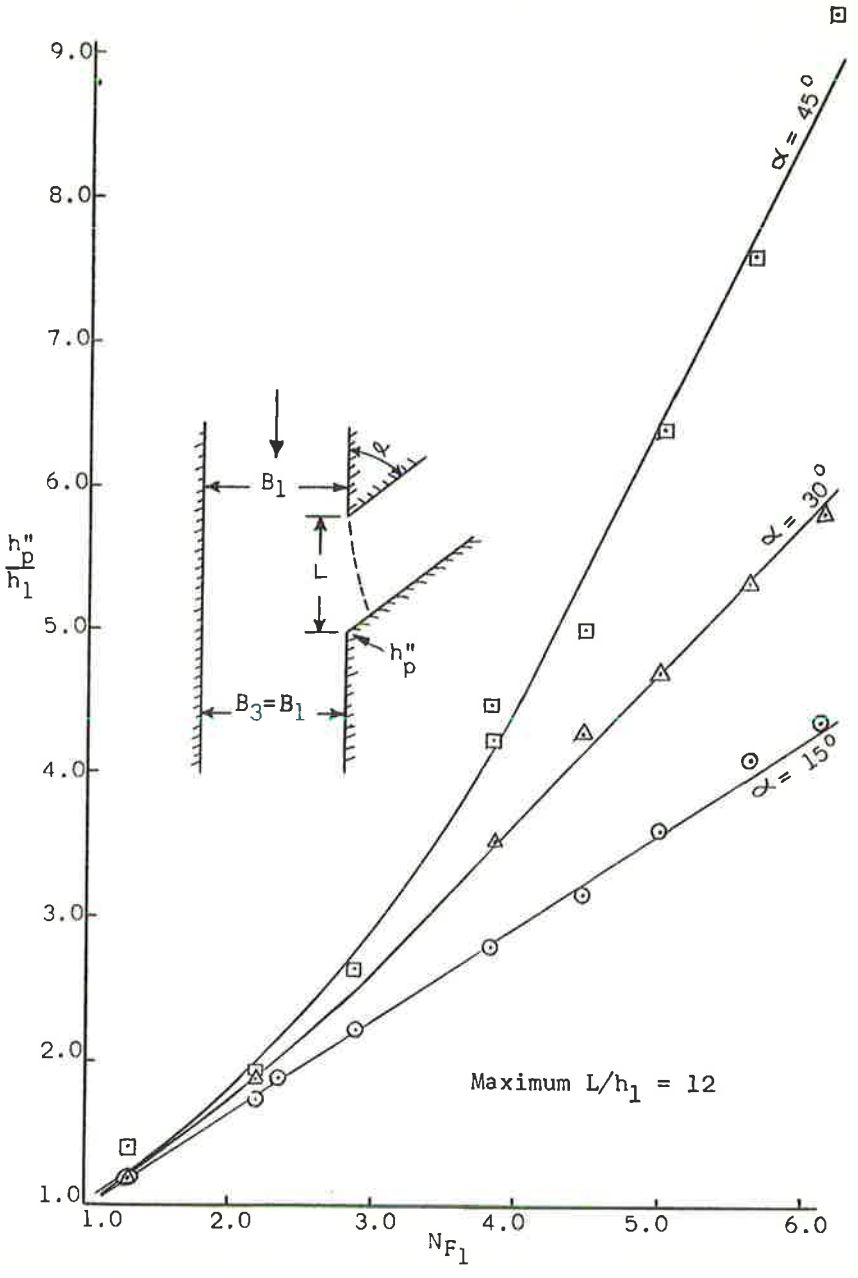

Figure 11. Pile-up at downstream corner of side channel for simple rectangular channel junctions when $Q_2 = 0$.

Experience in the laboratory with sloping channels has indicated that the angles are usually a few degrees less than those predicted by the analysis. This discrepancy, however, is small and it leads to conservative design.

With the value of β_1 known, Figure 9 can be entered to determine the wall pile-up height on the side of the main channel. The highest part of the pile-up occurs actually somewhat downstream from the point indicated by the angle β_1, and the wave is reflected

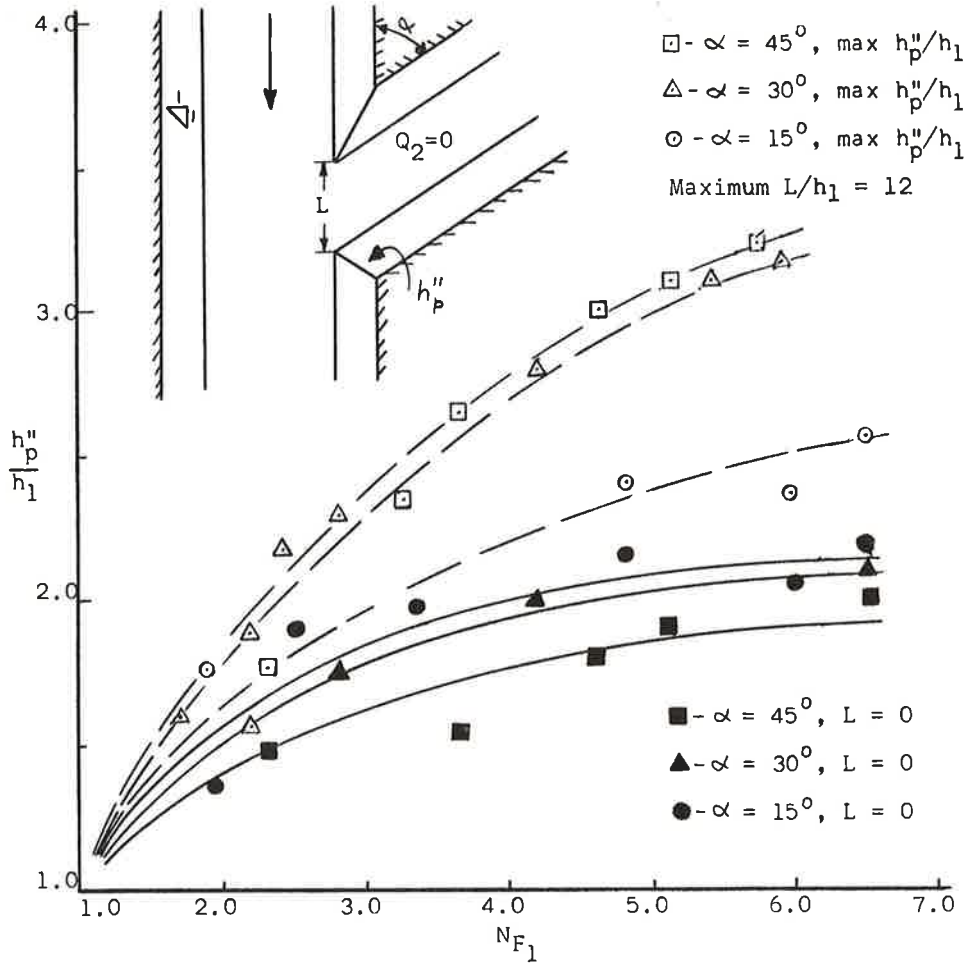

Figure 12. Plot of relative pile-up in trapezoidal channel junctions when $Q_2 = 0$; dashed lines indicate maximum observed h''_p/h_1 for all values of L studied; solid lines represent h''_p/h_1 for L = 0 (triangular side channel).

from side to side in the main channel, attenuating quite slowly. It is, therefore, necessary to design the main channel walls high enough to handle this first pile-up and subsequent reflections.

If the angle β_2 is less than the angle of incidence of the two channels, the diagonal wave, through which the side channel flow passes, does not intersect the wall of the side channel but passes harmlessly out into the main channel.

The designer must bear in mind that flows other than the design flows may occur in the channels. Laboratory experience indicates that conditions of zero flow in one channel and design flow in the other channel can create severe pile-up conditions. This can be quite serious if the junction has been designed to provide no pile-up in the side channel (β_2 less than α), because with no flow in the side channel and design flow in the main channel a good deal of pile-up may occur in the side channel.

Laboratory results of wall pile-up in the main channel resulting from flow from the side channel alone are summarized in Figure 10 for rectangular channels as well as for trapezoidal channels of 1:1 side slopes. Laboratory results indicating side channel wall pile-up with no flow in the side channel are shown by Figures 11 and 12.

Proper design considerations would include an investigation of design flow in both channels plus the possibilities of no flow in each channel while there is design flow in the other.

If the Froude numbers in the channels are small, there is the possibility of obtaining subcritical flow in the junction. In some cases this may be desirable because the diagonal waves extend across the channels at large angles and the supercritical flow problems do not exist. This point will not be discussed further here because this is a discussion of supercritical flow channel junctions.

CHANNEL JUNCTIONS WHICH MINIMIZE WALL PILE-UP PROBLEMS

Thus far, only the simple junction has been discussed. This type of junction is fraught with diagonal wave and pile-up problems which cannot be tolerated in many applications. The laboratory experiments of this study pointed the way toward what the authors feel is a rather complete solution to the pile-up problem. The principles involved in this solution are: (a) flow in the main channel should not be disturbed by

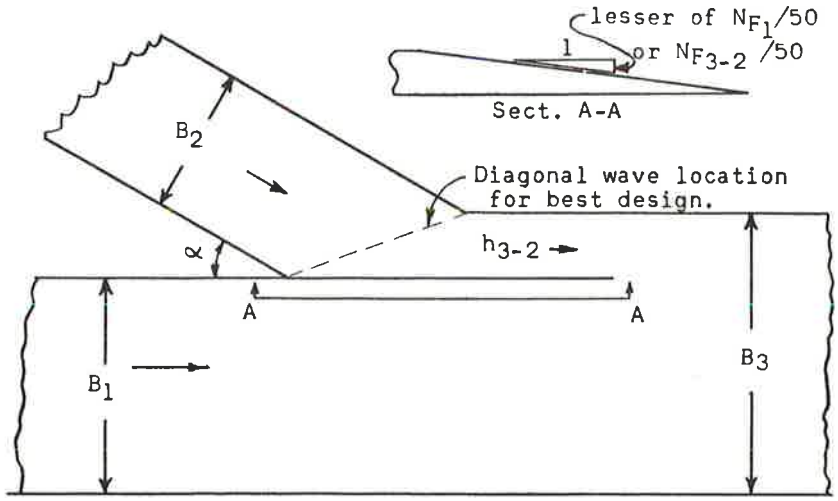

Figure 13. Sketch of improved rectangular channels junction.

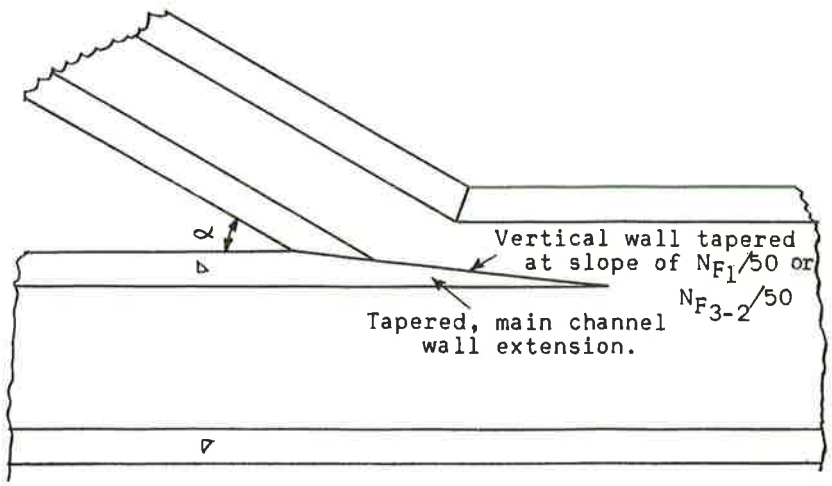

Figure 14. Sketch of improved trapezoidal channels junction; note that vertical wall has a vertical slope of the lesser of $N_{F_1}/50$ or $N_{F_{3-2}}/50$.

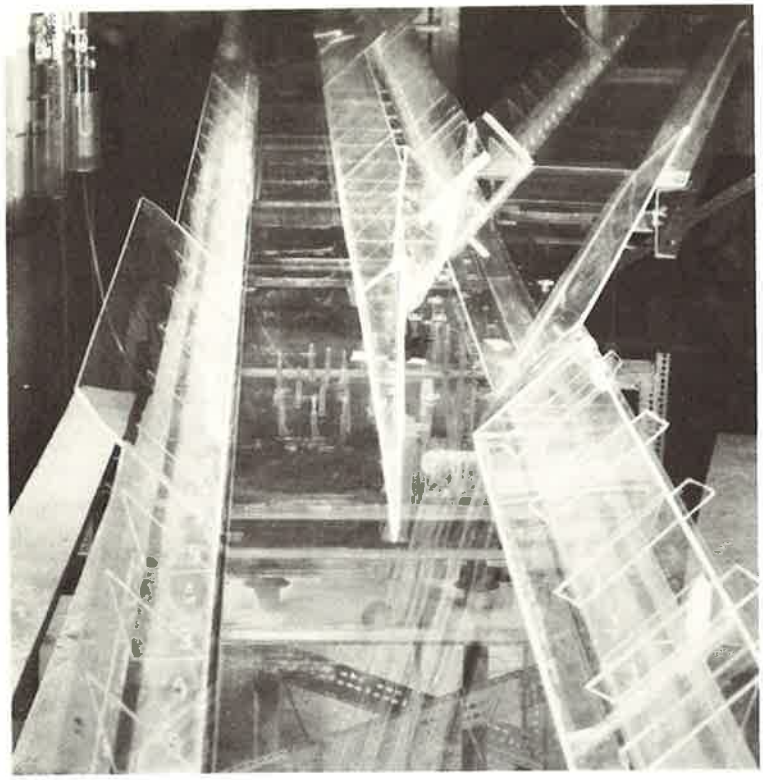

Figure 15. Improved junction of trapezoidal channels.

changes in direction of any kind, and (b) the direction of flow of the fluid entering from the side channel should be changed to that of the direction of the main channel without affecting the main channel flow.

An example of the proposed solution to the problem of wall pile-up is shown for a 15 deg, trapezoidal channel junction in Figures 13, 14, and 15. The salient features of the junction are as follows: the main channel is widened downstream from the junction to accommodate the sum of the main and side channel discharges; the side of the main channel on the side at which the side channel enters is gradually tapered in height but kept in the plane of the side of the main channel upstream; and the side channel flow is turned by means of a vertical, tapered wall placed parallel to the sides of the main channel for a rectangular channel or almost parallel for a trapezoidal main channel. One purpose of this tapered wall baffle arrangement is to remove the wall from the side of the main channel water gradually thus creating a gradual negative disturbance when the main channel flow is deeper than that entering beside it from the side channel (Fig. 16). With little or no side channel flow, gradual taper results in a gradual spilling of the main channel water against the widened side of the main channel just downstream from the side channel opening. This gradual spilling prevents a pile-up of any consequence on the main channel wall. With little or no main channel flow (Fig. 17), the side channel flow spreads in the main channel, but it enters the main channel in a downstream, rather than a cross channel, direction and does not pile-up on the main channel wall to a depth greater than the depth of design flow in the main channel.

With design flow in both channels (Fig. 18), the vertical wall still diverts the side channel flow into the direction of the main channel flow and the water surfaces of the main and side channel flows are also then matched. The side channel flow plus the tapered channel wall produce, then, the same hydrostatic pressure against the main channel flow as that of the channel wall just upstream from the junction. The main channel flow then experiences only a reduction in wall friction but no negative disturbance as it flows

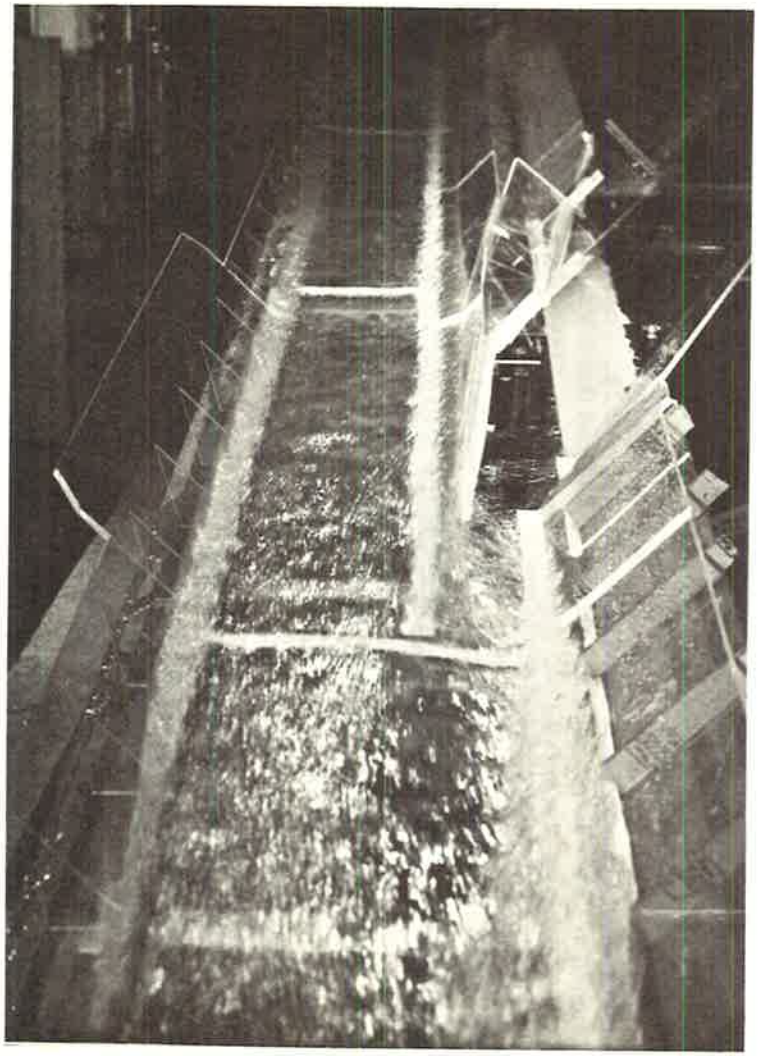

Figure 16. Flow from the main channel in an improved channel junction of trapezoidal channels; $N_{F_1} = 3.3$.

Figure 17. Flow from the side channel only, in the improved junction of Figure 16; $N_{F_2} = 2.6$.

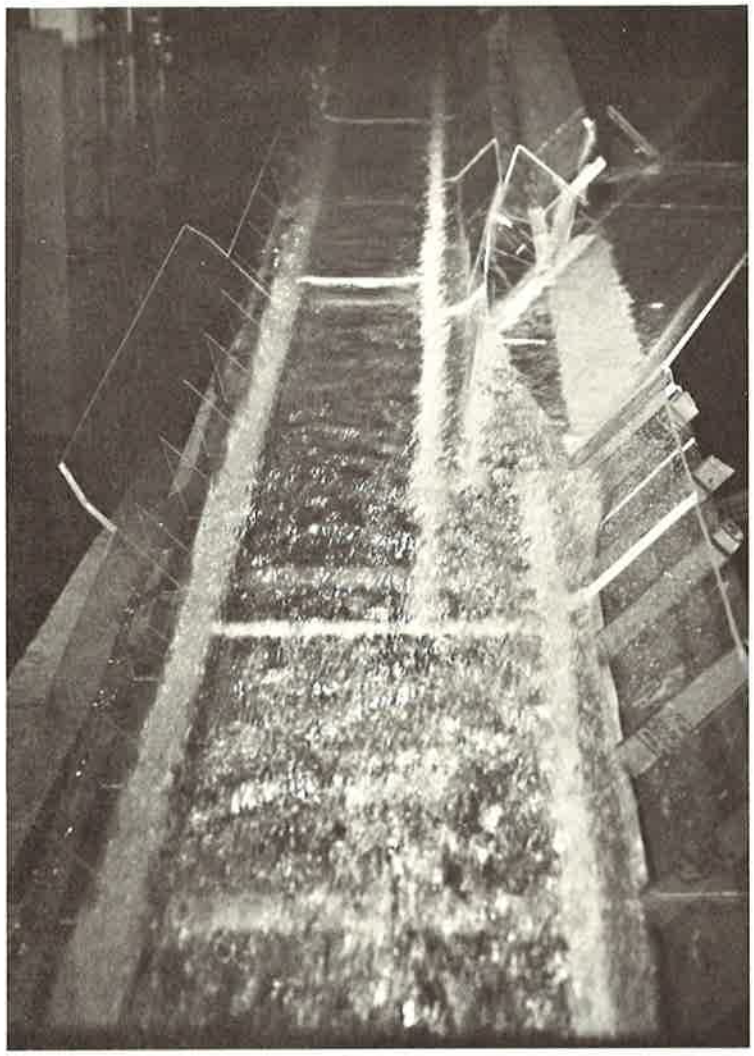

Figure 18. Design flows from both channels, in the improved junction of Figures 16 and 17; $N_{F_1} = 3.3$ and $N_{F_2} = 2.6$.

downstream. With no positive or negative disturbances impinging on the main channel flow, diagonal waves are not produced in this channel and the problem is eliminated.

In the laboratory experiments, the difference in velocity between the former side channel flow and the original main channel flow as the two begin to flow side by side in the new main channel section did not appear to create any kind of disturbance.

Though it was the original intent of the study to determine a solution to the diagonal wave problem only for rectangular channels, the solution found works equally well for trapezoidal and rectangular channels. The Froude number for trapezoidal channels, however, is defined as $V/(gh_m)^{1/2}$, where h_m is the mean depth in the channel defined by the ratio of channel cross-sectional area to the width of the channel at the water surface. With this change, Figures 3 and 9 still yield reasonable results.

Laboratory results indicate the following criteria should be met if the channel junction is to eliminate diagonal wave problems:

1. The channel downstream from the junction must be enlarged so that the depth of flow in the downstream channel is the same as in the main channel preceding the junction.

2. At design flow, the water surface of the flow from the side channel where it merges with the main channel flow must be at the same elevation as the main channel flow. If the water from the side channel is deeper than the main channel flow, a positive disturbance will be sent out into the main channel. If the water entering from the side channel is not as deep as in the main channel, there will be a negative disturbance created in the main channel flow. This ultimately results in a pile-up on the channel wall downstream from the junction.

3. If the flow in the side channel approaches the junction at an abrupt angle of incidence, as indicated in Figure 5, the diagonal wave required to change the direction of the side channel flow, must not strike the side channel wall, but should just strike the point of intersection of the side channel wall and the enlarged main channel wall. This eliminates wave problems on the wall of the side channel, and downstream in the main channel, from this source. However, since Froude numbers can seldom be predicted with complete accuracy in advance, it is wise to design according to the methods indicated here and then make provision for some pile-up along the downstream end of the side channel near the point of its intersection with the enlarged main channel.

4. Laboratory experiments indicate that the main channel on the side channel side of the junction, should be tapered as it extends from the upstream side of the junction, with a slope of no less than $N_{F_1}/50$ or $N_{F_{3-2}}/50$, which ever yields the smaller rate of taper to be most effective. $N_{F_{3-2}}$ is the Froude number of the flow from the side channel just downstream from the diagonal wave which forces that flow to change its direction to that of the main channel flow. $N_{F_{3-2}}$ instead of N_{F_2} enters the baffle design because the side channel flow which actually contacts the baffle is that which has changed direction and Froude number. $N_{F_{3-2}}$ is determined with the aid of Figure 3 and

$$N_{F_{3-2}} = \frac{h_2 B_2 \sin \beta_2}{h_1 (g h_{3-2})^{1/2} \sin (\beta_2 - \theta_2)} \tag{9}$$

which is derived simply from the continuity equation assuming the design depth of the side channel flow at the baffle to be the same as the design main channel depth, h_1.

If the preceding criteria are met, our laboratory experience indicates that the diagonal wave and pile-up problems are minimized or eliminated for the design flow in the channels. For less than design flow, diagonal waves exist, but they do not produce pile-ups which are greater than the depths of flow encountered for design flows.

The following design problem indicates that for given conditions in the main channel, the side channel must be designed to create the proper results. It is not possible to fit all combinations of side and main channel conditions to the criteria already enumerated.

Given:

Rectangular channels

$B_1 = 20$ ft, $h_1 = 5$ ft, $V_1 = 40$ ft/sec
$B_2 = 10$ ft, $h_2 = 2$ ft, $V_2 = 30$ ft/sec

Required:

Determine junction dimensions to minimize diagonal wave problems.

Solution:

$$N_{F_1} = \frac{V_1}{\sqrt{g h_1}} = \frac{40}{12.7} = 3.16$$

$$N_{F_2} = \frac{V_2}{\sqrt{gh_2}} = \frac{30}{8.02} = 3.74$$

Since the depth in the main channel must be maintained at 5 ft, h_3/h_2 for the side channel flow is 5/2. Entering Figure 3 with $N_{F_u} = 3.74$ and the depth ratio, $h_3/h_2 = 5/2$, $\beta_2 = 34$ deg and $\theta_2 = 19$ deg. Since only the side channel flow changes direction, $\alpha = \phi_2 = 19$ deg. $N_{F_{3-2}}$ is determined by means of Eq. 9.

$$N_{F_{3\ 2}} = \frac{h_2 V_2 \sin \beta_2}{h_1 (gh_{3-2})^{1/2} \sin (\beta_2 - \theta_2)} = \frac{(2)(30)(0.559)}{(5)(12.7)(0.259)} = 2.04$$

The taper of the main channel wall through the junction is sloped at the smaller of $N_{F_1}/50 = 3.16/50 = 0.0632$, or $N_{F_{3-2}}/50 = 2.04/50 = 0.0408$. The tapered side then is sloped at 0.0408 ft/ft, and, allowing one foot of freeboard, the length of the baffle is $(5 + 1)/0.0408 = 145$ ft long.

The downstream width of the main channel is

$$20 + \frac{10 \sin (34° - 19°)}{\sin 34°} = 24.62 \text{ ft, say } 24.6 \text{ ft.}$$

ACKNOWLEDGMENTS

This study was sponsored by the U. S. Bureau of Public Roads. The authors wish to express their appreciation to the Bureau for its sponsorship and to several of its engineers for their many constructive suggestions during the course of the project.

The authors also wish to acknowledge the valuable suggestions received from personnel of the U. S. Army Corps of Engineers hydraulic laboratory at Whittier Narrows, Calif., which helped greatly in the formulation of the study.

REFERENCES

1. Ippen, Arthur T. Mechanics of Supercritical Flow. High-Velocity Flow in Open Channels, A Symposium. ASCE Trans., Vol. 116, p. 268, 1951.
2. Ippen, Arthur T., and Harleman, Donald R. F. Verification of Theory for Oblique Standing Waves. ASCE Trans., Vol. 121, p. 678, 1956.
3. Rouse, Hunter, Bhoota, B. V., and Hsu, En-Yun. Design of Channel Expansions. High-Velocity Flow in Open Channels, A Symposium, ASCE Trans., Vol. 116, p. 347, 1951.
4. Behlke, Charles E. An Investigation of Supercritical Flow Channel Junctions. Eng. Exp. Sta., Oregon State Univ., 1964.

Generalized Hydraulic Characteristics of Grate Inlets

JOHN J. CASSIDY, Associate Professor of Civil Engineering, University of Missouri, Columbia

Five basic types of grate inlets were investigated. A rational qualitative analysis of the variables governing the efficiency of a grate inlet was verified through experimental measurement. The experimental results are presented in a generalized graphical fashion valid for any size grate. These plots can be used for design purposes, and a method is presented for determination of the length of grate required for operation at optimum efficiency.

The five basic types of grates are classified according to their decreasing hydraulic efficiencies. Grates constructed with curved-vane type bars were found to be the most efficient over the largest range of gutter velocities.

•SURFACE drainage of streets and urban highways is frequently accomplished through the use of curb inlets, grate inlets, or a combination of both. If drainage is to be accomplished in the most economical manner, the relative merits of each drainage device must be known. Curb inlets have the disadvantage of being inefficient flow interceptors unless used in conjunction with some form of gutter depression (1, 2). Use of depressed gutters is not a desirable practice on today's modern, high-speed roadways. Consequently, considerable attention has been focused on the hydraulic characteristics of grate inlets. Li, Goodell, and Geyer (2) have generalized hydraulic characteristics to the extent that they were able to investigate models at less than full scale. Through their generalized analysis, they were able to formulate approximate relationships for hydraulic design.

Larson and Straub (3) have made an attempt to generalize the results of experimental studies in terms of a "velocity index" $\sqrt{S_0}/n$ where S_0 is the longitudinal gutter slope and n is the Manning coefficient. However, their graphical results apply only to the size of grate investigated. They also conducted self-cleaning tests on their grates.

The investigation reported herein was conducted with the thought in mind that generalized hydraulic characteristics, independent of scale, provide the only firm means of comparing the operating efficiencies of two grates.

PHYSICAL CONSIDERATION OF THE FLOW

Flow over, through, and around any particular grate inlet is very complex at best. However, if consideration is given to the fluid, geometric, and flow variable involved, it is possible to clarify the picture to a large degree.

The variables which play a role in determining the efficiency of any grate are the following:

Q_0 = flow rate approaching the grate;
Q_i = flow rate intercepted by the grate;
ρ = density of the water;

Paper sponsored by Committee on Surface Drainage of Highways and presented at the 45th Annual Meeting.

γ = specific weight of the water;
W = width of the grate (normal to the flow);
L = length of the grate (parallel to the flow);
D = depth of flow upstream from the grate (in this case measured at the curb);
β = a dimensionless characteristic which will be assumed to completely describe the geometric configuration of the grate;
S = cross slope of the gutter; and
S_o = longitudinal slope of the gutter.

Functionally the variables are related by the expression

$$Q_i = f(Q_o, \rho, \gamma, W, L, D, \beta, S, S_o) \tag{1}$$

If the technique of dimensional analysis is applied to Eq. 1, the functional relationship can be changed to

$$\frac{Q_i}{Q_o} = \phi\left(\frac{Q_o}{\sqrt{\frac{\gamma}{\rho}D}}, \frac{L}{D}, \frac{D}{W}, \beta, S, S_o\right) \tag{2}$$

In Eq. 2, the leftmost term inside the parentheses is in actuality the Froude number of the approaching flow and can be written without reduction in generality as $V_o/\sqrt{gD}$ (4). The term Q_i/O_o is the efficiency of the grate. Evidently the efficiency of the grate will be influenced by the Froude number of the approaching flow, the relative length of the grate L/D, the relative depth of flow D/W, the cross slope S, the longitudinal slope S_o, and the geometric configuration of the grate β. All the parameters in Eq. 2 are dimensionless and are therefore applicable regardless of the absolute size of the grate or the dimensional units used.

The role of the Froude number is qualitatively clear. For any given depth, the faster the flow, the greater the tendency for water to bypass or jump over the grate. Hence, efficiency can be expected to decrease with increasing $V_o/\sqrt{gD}$.

Relative length of the grate is known to be important. For a given length of grate, a wide grate will intercept more flow than a narrow grate. Hence, efficiency will increase with a decrease in L/W (certain limits can be expected to occur).

For a given Froude number, efficiency of a grate will be decreased with an increase in relative depth D/W because more flow can then be expected to go around and over the grate.

The role of the geometry is somewhat more complicated. The shape of the grate as well as the shape, spacing, number, thickness, and orientation of the bars is all assumed to be included in the parameter. Obviously more than one parameter would be needed to completely describe the configuration of the grate.

Eq. 2 indicates a qualitative relationship between the variables influencing the hydraulic efficiency of any grate. Although understanding of fluid flow made it possible to predict certain behavior, an experimental study must ultimately be carried out to obtain the quantitative relationships necessary for design purposes.

EXPERIMENTAL APPARATUS AND PROCEDURES

Incorporation of the alternate form of the Froude number transforms Eq. 2 to

$$\frac{Q_i}{Q_o} = \phi\left(\frac{V_o}{\sqrt{gD}}, \frac{L}{D}, \frac{D}{W}, \beta, S, S_o\right) \tag{3}$$

To investigate experimentally the functional relationship indicated by Eq. 3, it is necessary to have independent control over all variables except the dependent variable

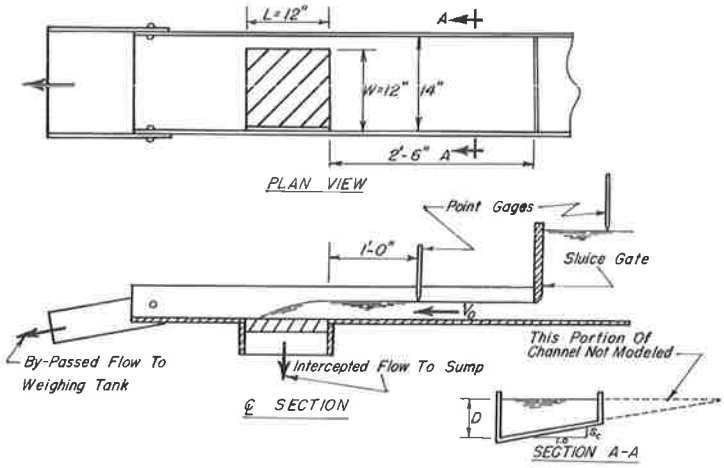

Figure 1. Experimental apparatus.

Q_i/Q_o. Other experimenters have set a particular slope S_o and then varied the discharge Q_o. Such a procedure does not provide absolute control over the depth of flow, because it is dependent on the cross slope, the longitudinal slope, the boundary roughness, and the discharge rate. To investigate the effect of S_o alone, it was obviously necessary to provide independent control of both $V_o/\sqrt{gD}$ and D/W. Such control was established by discharging water under a sluice gate into the gutter. The bottom of the sluice gate was cut in such a fashion that flow under the sluice gate occurred with a level free-surface and without contraction. Depth of flow was controlled by adjusting the sluice gate opening, and the velocity of flow was controlled by the head maintained. Discharge rate upstream from the gate was measured with a calibrated venturi meter. The discharge not intercepted by the grate (Q_o - Q_i) was directed into a weighing tank.

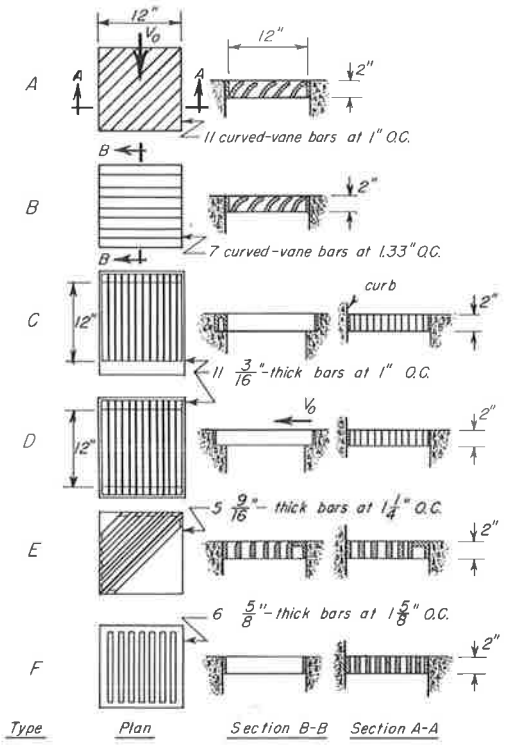

Figure 2. Grate configuration.

Cross slope of the gutter was set by tilting the entire flume about its longitudinal axis, while the longitudinal slope was set by rotating the flume about a transverse axis. Sluice gates with the proper bottom slope were utilized for each different cross slope. Depth of flow was measured with a point gage at a point 1.0 ft upstream from the grate. Arrangement of the experimental apparatus is shown in Figure 1.

Six different grate geometries were studied experimentally. The proportions of these grates are shown in Figure 2. Procedure was identical for each grate:

1. The sluice-gate opening was set to produce a particular depth of flow.

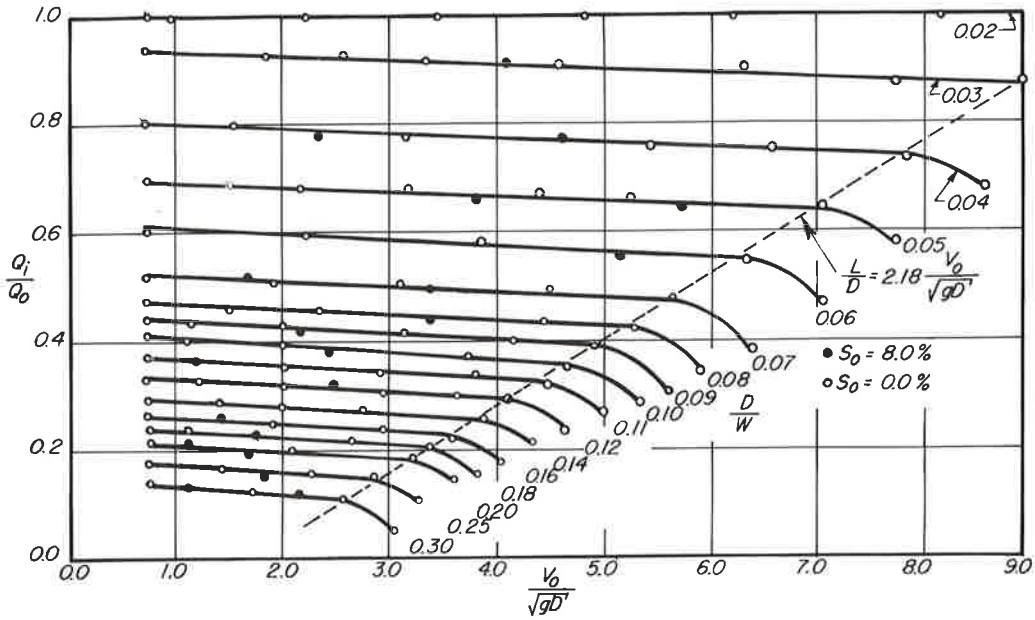

Figure 3. Type A grate, 50.0 to 1.0 cross slope.

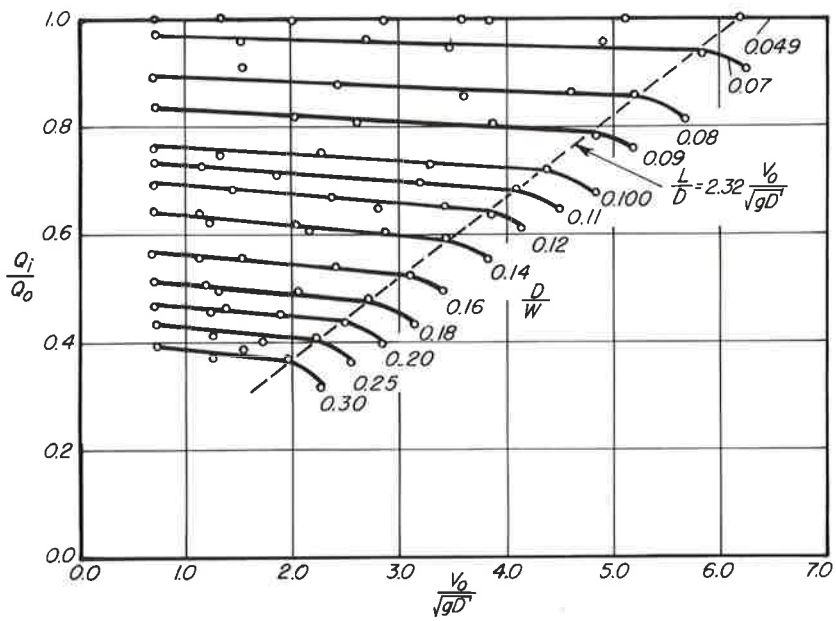

Figure 4. Type A grate, 20.6 to 1.0 cross slope.

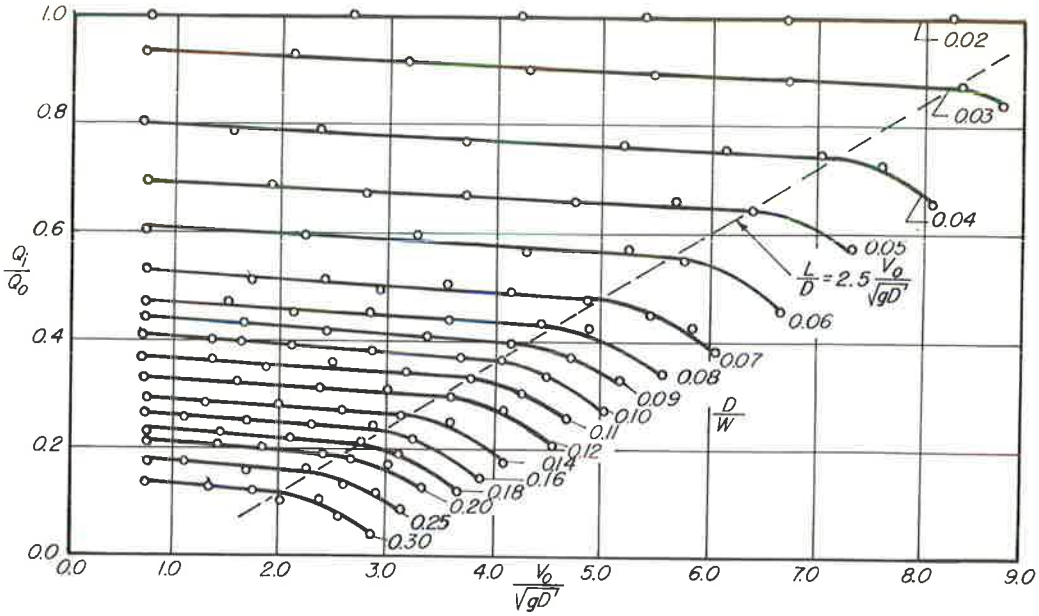

Figure 5. Type B grate, 50.0 to 1.0 cross slope.

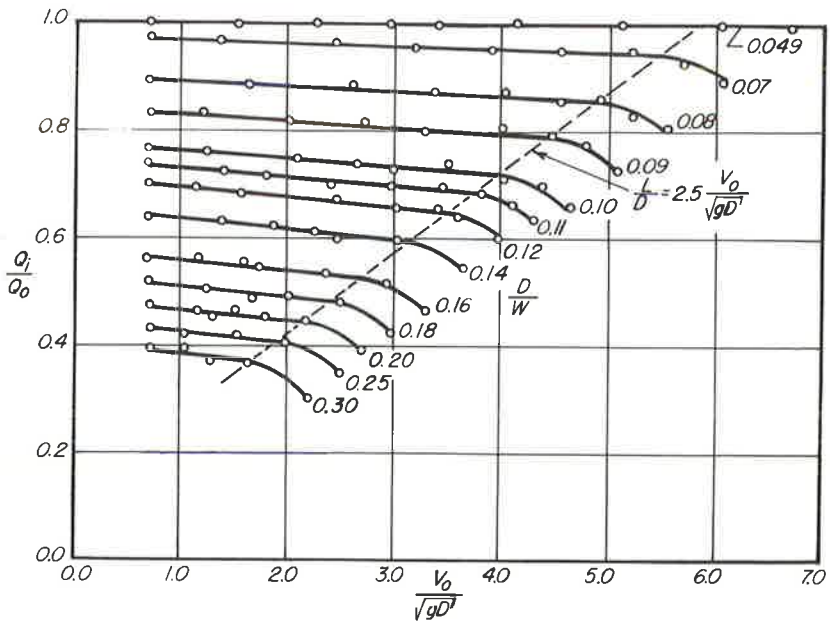

Figure 6. Type B grate, 20.6 to 1.0 cross slope.

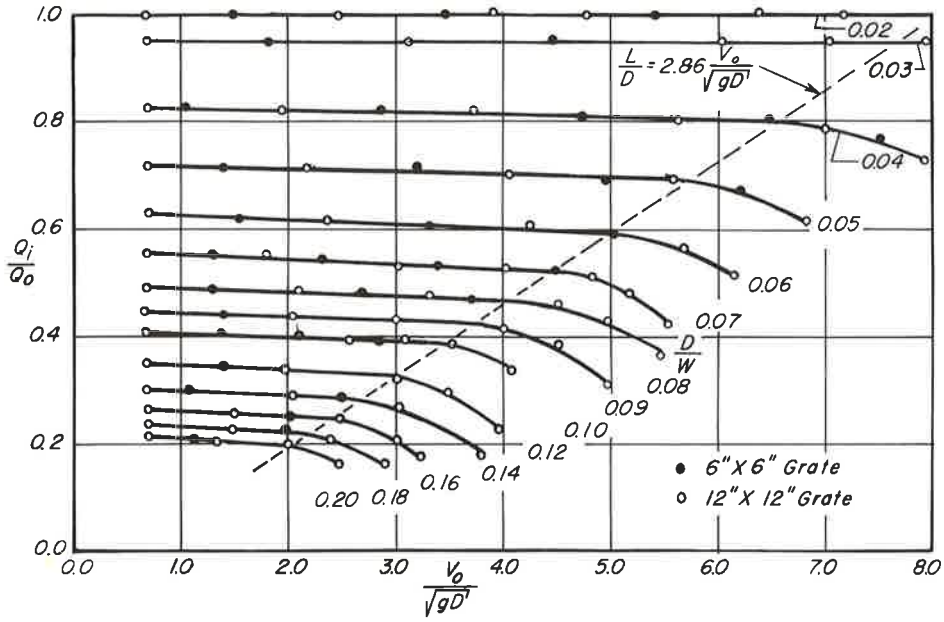

Figure 7. Type D grate, 50.0 to 1.0 cross slope.

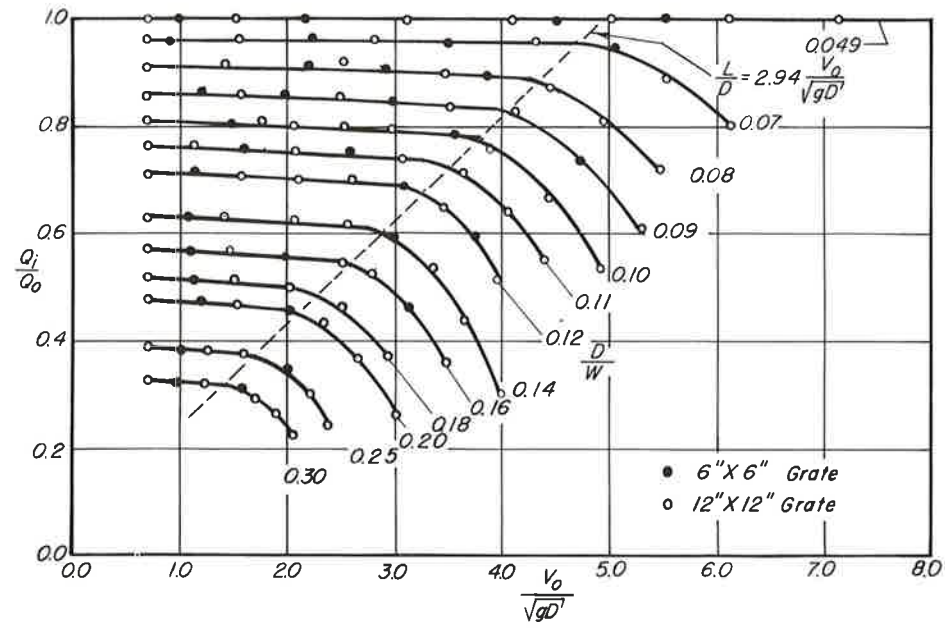

Figure 8. Type D grate, 20.6 to 1.0 cross slope.

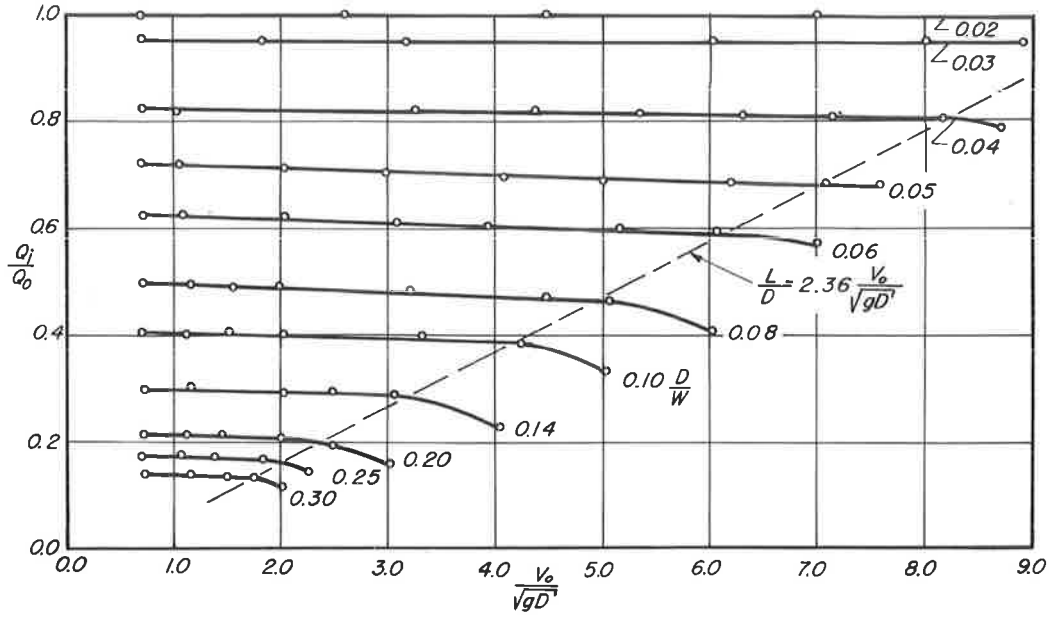

Figure 9. Type C grate, 50.0 to 1.0 cross slope.

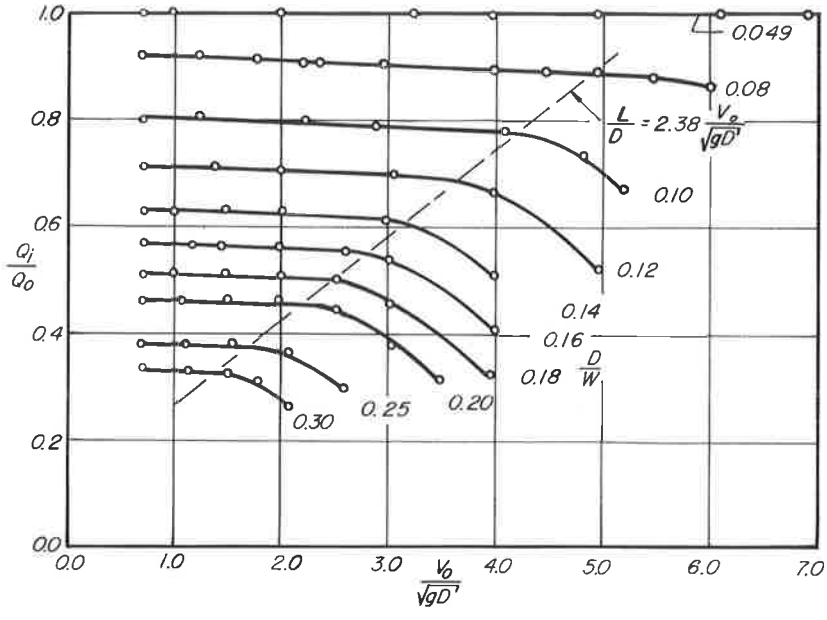

Figure 10. Type C grate, 20.6 to 1.0 cross slope.

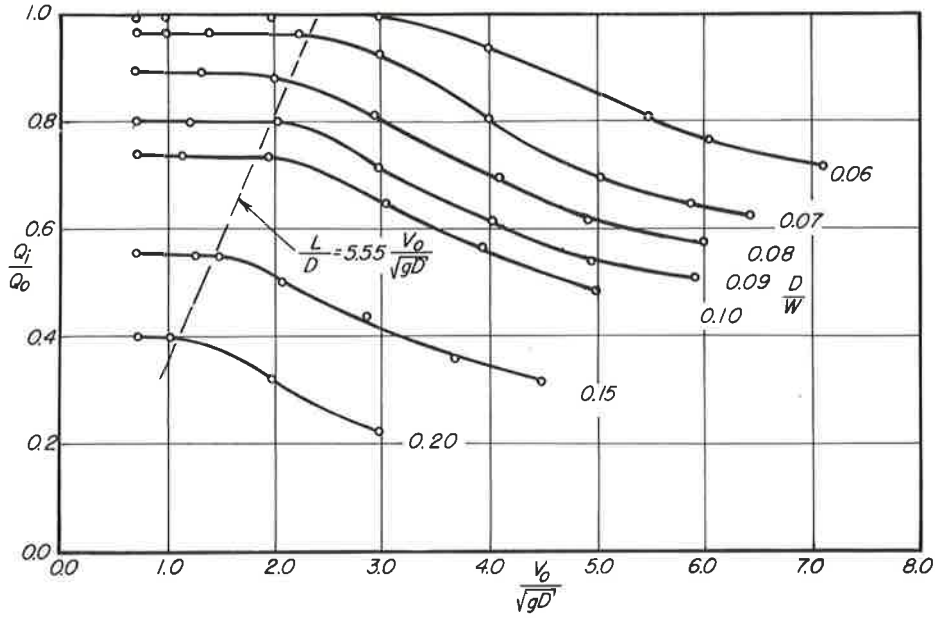

Figure 11. Type E grate, 20.6 to 1.0 cross slope.

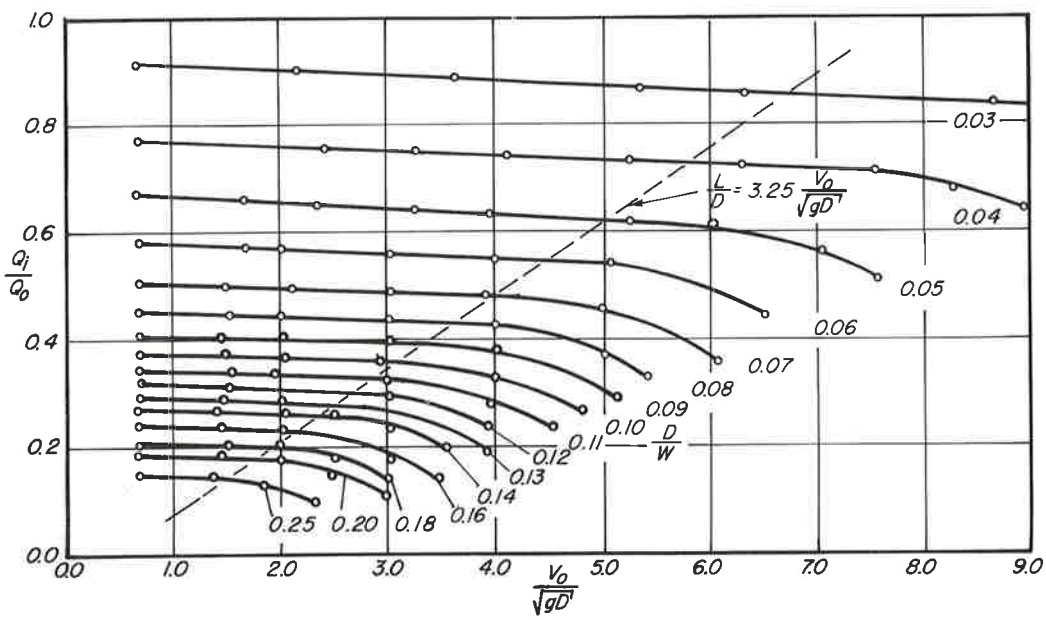

Figure 12. Type F grate, 50.0 to 1.0 cross slope.

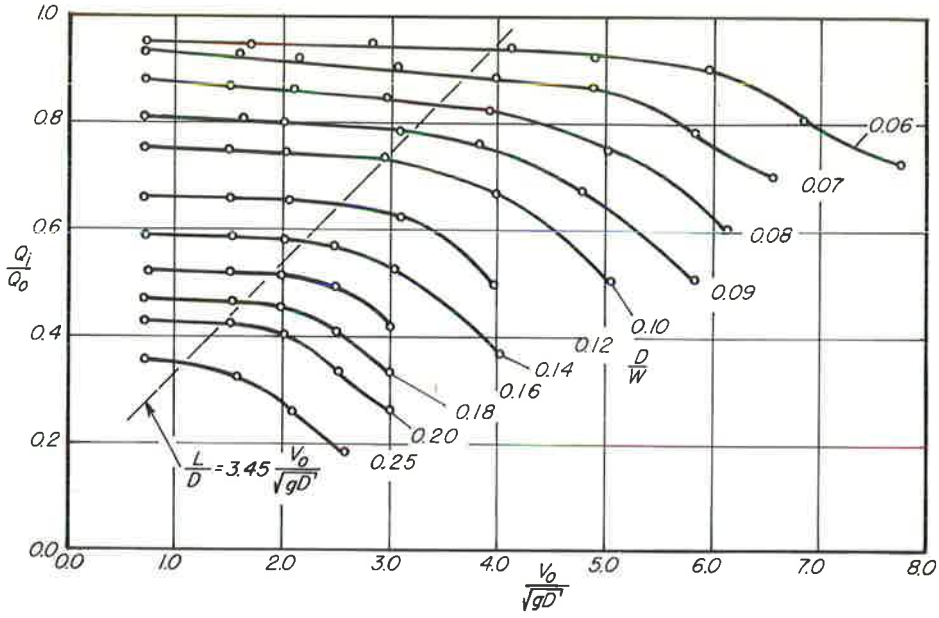

Figure 13. Type F grate, 20.6 to 1.0 cross slope.

2. Flow rate was adjusted to produce a particular Froude number.
3. The flow not intercepted was weighed.
4. The three foregoing steps were repeated for each of two cross slopes for each grate.

Experimental results for the six grates are shown in Figures 3 through 13. Because each grate was 1.0-ft square, the ratio L/W = 1.0 in every case. Cross slopes of 20.6 to 1 and 50 to 1 were used for each grate.

RESULTS

Hydraulic Characteristics

It was possible to eliminate the longitudinal gutter-slope from the parameters involved in Eq. 3. Actually the longitudinal slope plays an important role in determining the average velocity of flow in the gutter. Unless the gutter is on an extremely steep slope (for instance, 45 degrees), it might well be expected that the longitudinal slope would play a minor role in determining the grate efficiency. This hypothesis was checked experimentally at the outset of the program. Grate A was studied on a zero slope and again on an 8 percent slope. No noticeable change in characteristics was observed (Fig. 3). Therefore, in all of the remaining experiments, a horizontal gutter was used.

A flume with a 14-in. width was used to represent the gutter. Because the grates used were only 12 in. wide, a triangular flow section was obtained only for small depths. To compute the grate efficiency, it was assumed that flow would take place at average velocity in the imaginary portion of the triangular cross-section (Fig. 1). This is obviously an approximation because both viscous and surface tension effects will be important in the actual triangular section. However, the average velocity in the triangular portion of an actual highway gutter would, without question, be somewhat lower than was assumed herein because of increasing importance of viscous forces with decreasing depth. From the design standpoint, the assumption made here was assumed to be conservative. The validity of this assumption was investigated experimentally. A grate, geometrically similar to Grate C but only half the size (6 in. by 6 in.), was constructed and tested in the 14-in. wide flume. Hence, a triangular flow cross-section was obtained for a value of D/W twice as large as that for the 12-in. square grate. The experi-

mental results (Figs. 7 and 8) indicate that the magnitude of the error in efficiency produced by assuming that flow would occur at average velocity in the triangular section is negligible. This reduced scale model also verified that the efficiency was truly a function of the variables indicated in Eq. 3.

Two distinctly different flow patterns were observed for each grate (Figs. 3 through 13). At relatively low values of the relative depth D/W or the Froude number $V_o/\sqrt{gD}$, no flow crossed over the grate and the flow pattern was smooth. Eventually, as either the relative depth or the Froude number is increased, the flow strikes the downstream side of the grate creating a violent disturbance—not unlike a hydraulic jump—on the grate itself. Once the disturbance is formed, flow begins to pass directly over the grate and the efficiency Q_i/Q_o is accordingly reduced rather abruptly. The onset of the disturbance is indicated (Figs. 3 through 13) by the point at which the efficiency curves bend abruptly downward.

As long as flow does not pass directly over the grate, the length of the grate has only a minor effect on efficiency. For a long grate, as opposed to a short one, more flow enters the grate from the roadway. However, Li et al. (2) have shown that this contribution to the intercepted flow is quite small unless the grate is depressed.

The dotted line (Figs. 3 through 13) indicates the limiting condition at which a hydraulic jump will form and water will begin to flow directly over the grate. An approximate equation was formed for each of these lines and is shown on the graphs. Each of the equations has the form

$$\frac{L}{D} = m \frac{V_o}{\sqrt{gD}} \tag{4}$$

The magnitude of m is an indication of the grate's efficiency. Large values of m indicate that a hydraulic jump forms readily, while a small value indicates the opposite trend. Grates with a small value of m are obviously the most desirable because the value of m is directly proportional to the length of grate required to insure maximum efficiency of operation at high flow rates.

Eq. 4 is of further use to the designer. Rewritten as $L = Dm(V_o/\sqrt{gD})$, Eq. 4 yields the length of grate required to eliminate flow passing directly over the grate for gutter flow at given values of depth and Froude number.

Although the experiments conducted in this study were performed on square grates, Figures 3 through 13 are applicable for any grate with similar bar design, regardless of size, as long as the length of the grate is not less than that given by Eq. 4.

Observation of the dimensionless plots shows that grates utilizing curved vane-type bars[1] are of the most efficient type (Grates A and B). At low values of $V_o/\sqrt{gD}$, the efficiency of a grate with narrow, widely-spaced longitudinal bars (Grate C) is essentially the same as ones formed with curved vanes, but curved vane bars are more effective in preventing the formation of a hydraulic jump. Hence, the range of maximum efficiency is extended through use of the vane-type bars. Further evidence of the benefits of properly shaping the vanes is obtained by a comparison of efficiency curves for Grates A and E.

Grates with closely-spaced, relatively wide, flat bars (Grate F) are inefficient in the entire range (Figs. 12 and 13). Considerable flow follows the bars and passes directly over the grate prior to the formation of a hydraulic jump. In fact, the hydraulic jump is drowned out virtually as soon as it forms and the grate operates as an orifice.

A comparison of Figures 3 and 4 (Grate A) with Figures 5 and 6 (Grate B) shows that sloping of vanes has only a small effect on the efficiency of the grate, with the maximum efficiency being obtained for vanes placed at 45 degrees to the direction of flow.

In general, the hydraulic jump is formed when flow strikes the downstream side of the grate and rebounds upward. The range of efficient operation of Grate D was extend-

[1]The use of such bars in a highway grate has been patented.

ed greatly by the slight revision required to produce Grate C. Clear opening is the same in each case but the hydraulic jump forms much more readily on Grate C. The revision is a minor one, but highly desirable.

Application to Design

All of the experimental results (Figs. 3 through 13) could have been set forth in dimensional plots on which the intercepted flow rate Q_i was plotted against average gutter velocity V_o; individual curves would have been obtained for each separate value of D. A separate graph would then have been required for each size of grate tested as well as for each separate cross slope used. However, by plotting the curves in dimensionless form a graph is obtained which is valid for any size of grate because no absolute quantities appear in any of the plotted parameters. Both forms of plotting are equally useful in design, but the dimensionless form is the most compact.

To use the dimensionless graphs, the designer simply combines his calculated or known independent variable, V_o, W, D, to form the equivalent dimensionless parameters, $V_o/\sqrt{gD}$, D/W, used on the graphs. An example problem is presented in the Appendix to illustrate the use of the dimensionless plots for design purposes.

CONCLUSION

From the results of this investigation, the following conclusions can be made with regard to the operating characteristics of grate inlets:

1. The absolute hydraulic characteristics of any two grate inlets can be compared if the results of experimental tests are generalized according to the expression

$$\frac{Q_i}{Q_o} = \phi \quad \frac{V_o}{\sqrt{gD}}, \frac{D}{W}, \frac{L}{D}, S \ .$$

2. For all practicual purposes the efficiency of any grate inlet is not a function of the longitudinal gutter slope if the slope is less than 8 percent. However, the slope plays an important role in determining the average flow velocity.

3. The curves of efficiency vs Froude number and relative depth presented herein may be used for proportioning or spacing grate inlets.

ACKNOWLEDGMENTS

Phases of the investigation reported herein were supported by the University of Missouri Engineering Experiment Station and the Rowland Engineering Company, St. Louis, under a grant and an agreement, respectively. David Smith, Chi Hu, Albert Farrington, and Champal Patel, Research Assistants in the Department of Civil Engineering, University of Missouri, contributed at various times to the performance of the experiments and subsequent data analysis.

REFERENCES

1. Izzard, Carl F. Tentative Results on Capacity of Curb Opening Inlets. HRB Research Report No. 11-B, p. 36, 1950.
2. Li, Wen-Hsiung, et al. The Design of Storm-Water Inlets. The Johns Hopkins University, Baltimore, 1956.
3. Larson, C. L., and Straub, L. G. Grate Inlets for Surface Drainage of Streets and Highways. Bull. No. 2, St. Anthony Falls Hydraulics Lab., Univ. of Minn., June 1949.
4. Rouse, H., (Ed.). Engineering Hydraulics. John Wiley and Sons, New York, 1950.
5. Izzard, Carl F. Hydraulics of Runoff from Developed Surfaces. HRB Proc., Vol. 26, p. 150, 1946.

Appendix

EXAMPLE DESIGN PROBLEM

During the peak period of a design storm, runoff enters a gutter at the rate Q_e = 0.004 cfs per ft. The roughness of the gutter corresponds to a Manning's n equal to 0.02. Determine the required length and spacing of Type A gratings in order that gutter flow will not spread more than 8.0 ft toward the centerline. Longitudinal slope of the gutter is 4.0 percent and cross slope is 2.0 percent.

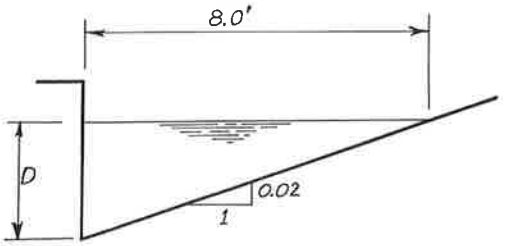

Figure 14. Gutter section at maximum depth.

Assume W = 2.0 ft

D (maximum depth) = 8(.02) = 0.16 ft

A (Flow area) = $0.16 \; \frac{8.0}{2} = 0.64 \text{ ft}^2$

To determine the discharge Q_o at depth D, use the relationship proposed by Hicks (5):

$$Q_o = 0.56 \left(\frac{Z}{n}\right) S^{1/2} D^{8/3}$$

where Z = 1/S.

Thus,

$Z = \frac{1}{S} = \frac{1}{0.02}$

(Cross Slope)

2500 .2

$$Q_o = 0.56 \left(\frac{50}{0.02}\right) (0.04)^{1/2} (0.16)^{8/3} = 2.11 \text{ cfs}$$

$$V_o = \frac{Q_o}{A} = \frac{2.11}{0.64} = 3.30 \text{ fps}$$

$$\frac{V_o}{\sqrt{gD}} = \frac{3.30}{\sqrt{32.2(0.16)}} = 1.45$$

$$\frac{D}{W} = \frac{0.16}{2.0} = 0.08$$

From Figure 3

$$\frac{Q_i}{Q_o} = 0.46$$

$$Q_i = 0.46(2.11) = 0.973 \text{ cfs}$$

$$\text{Spacing} = \frac{Q_i}{Q_e} = \frac{0.973}{0.004} = \underline{\underline{243 \text{ ft}}}$$

$$L = D(2.18)\frac{V_o}{\sqrt{gD}} = 0.16(2.18)(1.45) = \underline{\underline{0.50\ \text{ft}}}$$

If the grates are constructed with a length of 0.50 ft and a width of 2.0 ft, their hydraulic characteristics will be as shown to the left of the diagonal line in Figure 3 regardless of the fact that the corresponding ratio L/D = 0.25 instead of 1.0.